Dietary Emulsifiers Directly Impact Adherent-Invasive E. coli Gene Expression to Drive Chronic Intestinal Inflammation

Emilie Viennois, Alexis Bretin, Philip Dubé, Alexander Maue, Charlène J.G. Dauriat, Nicolas Barnich, Andrew Gewirtz, Benoit Chassaing

Dietary emulsifiers directly impact adherent-invasive *E. coli* gene expression to drive chronic intestinal inflammation

Emilie Viennois[1,2,3], Alexis Bretin[1], Philip E. Dubé[4], Alexander C. Maue[4], Charlène Dauriat[3,5] Nicolas Barnich[6], Andrew T. Gewirtz[1] and Benoit Chassaing[1,3,5,7,8]

[1] Institute for Biomedical Sciences, Center for Inflammation, Immunity and Infection, Digestive Disease Research Group, Georgia State University, Atlanta, GA, USA

[2] INSERM, U1149, Center of Research on Inflammation, Paris, France

[3] University of Paris, Paris, France.

[4] Taconic Biosciences Inc, Rensselaer, NY

[5] INSERM, U1016, team "*Mucosal microbiota in chronic inflammatory diseases*", Paris, France.

[6] Université Clermont Auvergne/Inserm U1071; USC-INRA 2018, Microbes, Intestin, Inflammation et Susceptibilité de l'Hôte (M2iSH), Clermont-Ferrand, France

[7] Neuroscience Institute, Georgia State University, Atlanta, GA

[8] Corresponding author and lead contact

Running Title: AIEC mediate emulsifier detrimental effects.

Corresponding Authors:
Benoit Chassaing, Ph.D.
INSERM, U1016, team "*Mucosal microbiota in chronic inflammatory diseases*"
Paris, France
E-Mail: benoit.chassaing@inserm.fr

Lead Contact
Benoit Chassaing, Ph.D.
INSERM, U1016, team "*Mucosal microbiota in chronic inflammatory diseases*"
Paris, France
E-Mail: benoit.chassaing@inserm.fr

Abbreviations: ASF, altered Schaedler flora; CMC, carboxymethylcellulose; IL-10, interleukin-10; P80, polysorbate-80; IBD, inflammatory bowel disease.

SUMMARY

Dietary emulsifiers carboxymethylcellulose (CMC) and Polysorbate-80 (P80) disturb gut microbiota, promoting chronic inflammation. Mice with minimal microbiota are protected against emulsifiers effects, leading us to hypothesize that these compounds might provoke pathobionts to promote inflammation. Gnotobiotic WT and IL10$^{-/-}$ mice were colonized with Crohn's disease-associated adherent-invasive *E. coli* (AIEC) and subsequently administered CMC or P80. AIEC colonization of GF and ASF mice results in chronic intestinal inflammation and metabolism dysregulations when consuming emulsifier. In IL10$^{-/-}$ mice, AIEC mono-colonization results in severe intestinal inflammation in response to emulsifiers. Exposure of AIEC to emulsifiers *in vitro* increase its motility and ability to adhere to intestinal epithelial cells. Transcriptomic analysis reveal that emulsifiers directly induce expression of clusters of genes that mediate AIEC virulence and promotion of inflammation. To conclude, emulsifiers promote virulence and encroachment of pathobionts, providing a means by which these compounds may drive inflammation in hosts carrying such bacteria.

Key Words: Emulsifier, adherent-invasive *Escherichia coli*, intestinal inflammation, flagellin.

INTRODUCTION

Intestinal inflammation is a central feature of many of the chronic inflammatory diseases that are increasingly afflicting developed, and developing, countries. For example, inflammatory bowel diseases (IBD), which include Crohn's disease and ulcerative colitis, and whose central defining feature is histopathologically-evident intestinal inflammation, has steadily increased since the mid-20th century and now afflicts more than 20 million people worldwide (Ng et al., 2017). Moreover, it is increasingly appreciated that low-grade intestinal inflammation, is associated with, and promotes, a variety of other chronic disease states including colon cancer and metabolic syndrome, whose features include obesity and dysglycemia (Cani et al., 2012; Chassaing and Gewirtz, 2014, 2016). Determinants of chronic intestinal inflammation include host genetics and gut microbiota composition, with IBD requiring a genetic predisposition to disease development (Xavier and Podolsky, 2007). In contrast, metabolic syndrome and colon cancer are associated with, and promoted by, microbiota dysbiosis in a wide variety of host genetic backgrounds (Arthur et al., 2012; Vijay-Kumar et al., 2010). While microbiota dysbiosis associated with gut inflammation is itself complex and varied, it frequently involves decreased in the abundance of some phyla, together with a greater relative abundance in Enterobacteriaceae (Chassaing and Darfeuille-Michaud, 2011). One specific bacteria associated with gut inflammation, particularly IBD is a pathovar of *Escherichia coli* (*E. coli*) named Adherent-invasive *E. coli* (AIEC) (Darfeuille-Michaud et al., 2004; Palmela et al., 2018). AIEC is implicated in the pathology of Crohn's disease, especially by its ability to adhere to and invade intestinal epithelial cells through expression of numerous virulence factors (Barnich et al., 2004; Barnich et al., 2007; Chassaing et al., 2011b; Glasser et al., 2001; Rolhion et al., 2007).

Development of gut inflammation is also influenced by diet, at least in part as a result of the influence of diet on gut microbiota composition (Laudisi et al., 2018; Nickerson et al., 2014; Nickerson and McDonald, 2012; Rodriguez-Palacios et al., 2018; Suez et al., 2014; Tobacman, 2001), with various elements of macronutrient content influencing microbiota and proneness to development of gut inflammation (Chassaing et al., 2015c; Llewellyn et al., 2018; Miles et al., 2017). Additionally, some food additives can promote gut inflammation. For example, and centrally relevant to this study, carboxymethylcellulose (CMC) and Polysorbate 80 (P80), which are commonly used synthetic emulsifiers that are added to a variety of processed foods to enhance texture and extend shelf-life, alter microbiota in a manner that promotes intestinal inflammation. More specifically, we have shown that administration of CMC or P80 to mice resulted in microbiota encroachment into the mucus, alterations in microbiota composition, including an increase of bacteria that produced pro-inflammatory flagellin and LPS, and development of chronic inflammation (Chassaing et al., 2015b; Chassaing et al., 2017b; Viennois and Chassaing, 2018). Such inflammation was associated with low-grade inflammation and metabolic syndrome in WT mice and increased incidence/severity of colitis in genetically susceptible mice (interleukin-10 (IL-10)$^{-/-}$) (Chassaing et al., 2015b). Furthermore, emulsifier consumption increased the susceptibility of mice to developing colonic tumors by creating and maintaining a proinflammatory environment associated with an altered proliferation/apoptosis balance (Viennois et al., 2017). While precise determination of emulsifier exposure in humans is challenging, average consumption of CMC and P80 are 46 and 8.2 mg/kg/bw/day in the United Kingdom, respectively (Cox et al., 2020; EFSA, 2015, 2017). Although average intakes in humans appear lower than doses we previously used in mouse models, our animal studies employed relatively short-term emulsifier exposure (Chassaing et al., 2015b; Chassaing et al.,

2017b) and the chronic nature of human intake over many years might allow to reach similar exposure levels. Moreover, we previously investigated the impact of these compounds individually, while processed food often simultaneously contain multiple dietary emulsifiers with, likely, additive or synergistic effects (Chassaing et al., 2015b; Chassaing et al., 2017b; Cox et al., 2020). While results from clinical trials on emulsifiers are not yet available, the observations that diets lacking emulsifiers and other suspected triggers of IBD are more effective than elemental diet in maintaining remission of pediatric CD highlights the importance of dietary triggers in IBD (Levine et al., 2019; Sabino et al., 2019).

That CMC and P80 did not induce low-grade gut inflammation or indices of metabolic syndrome in germ-free mice highlights that these compounds perturb host-microbiota homeostasis rather than directly trigger host pro-inflammatory gene expression (Chassaing et al., 2015b; Chassaing et al., 2017b; Viennois et al., 2017). Moreover, these compounds did not discernably impact mice harboring only a limited defined pathobiont-free microbiota, namely Altered Schaedler Flora (ASF) (Chassaing et al., 2017b), leading us to hypothesize that emulsifiers may not uniformly impact bacteria per se but rather provoke responses from pathobiont bacteria, particularly those, such as AIEC, that can induce virulence gene expression in response to select environmental conditions. Herein, we tested this hypothesis by administering CMC or P80 to gnotobiotic mice colonized by AIEC and, moreover, by directly examining the impact of these compounds on AIEC gene expression *in vitro*. We found that presence of AIEC was sufficient to make mice prone to the detrimental impacts of CMC and P80. Moreover, exposure to these compounds directly promoted AIEC virulence, as assessed by non-targeted transcriptomic analysis and ability to adhere to gut epithelial cells. These results

117 suggest that CMC and P80 might promote ability of pathobionts to colonize the intestine and
118 promote gut inflammation and its associated disease states.

RESULTS

AIEC confers proneness to detrimental effects of dietary emulsifiers

Administration of the dietary emulsifiers CMC and P80 to WT mice results in low-grade intestinal inflammation and metabolic syndrome (Chassaing et al., 2015b; Chassaing et al., 2017b). Such emulsifier-induced phenotypes were absent in germ-free mice as well as in ASF mice, which are colonized with a low complexity microbiota (Chassaing et al., 2017b), leading us to hypothesize that emulsifiers might promote gut inflammation by acting upon pathobiont bacteria that are present in many hosts. Hence, we investigated if addition of AIEC to ASF mice would render them prone to pro-inflammatory impacts of CMC and P80. ASF mice were colonized with AIEC reference strain LF82 (Darfeuille-Michaud et al., 2004), as outlined in **Figure S1A**, and the impact of emulsifier on intestinal inflammation and metabolism measured. ASF/AIEC mice administered either CMC or P80 displayed a range of features of intestinal inflammation, including increased colon weight, colon shortening, increases in colon weight/length ratio, as well as a non significant tendancy toward increased spleen weight and elevated levels of fecal lipocalin-2 (Lcn2) (**Figure 1A-G**). Such indices of inflammation were associated with increased intestinal expression of genes that promote and/or reflect inflammation (**Figure 1H-I and S1C-F**). Moreover, histological scoring of colonic sections indicated a significantly increased inflammation in CMC- and P80-treated mice compared with control animals (**Figure 1J and S1K**). Furthermore, such emulsifier-induced intestinal inflammation was associated with features of metabolic syndrome including elevations in body weight, fat pad mass, and fasting levels of blood glucose (**Figure 1 K-M**). Combination of all these morphological and molecular measurments of inflammation into principal coordinate analysis using Bray-Crutis distance showed a clear and significant clustering of CMC- and P80-treated

142 animals compared with control animals, further highligting the increase in inflammation level in
143 emulsifier treated mice (**Figure S1G**). Together, these data indicate that, like conventional mice,
144 and in contrast to ASF mice, which are fully protected against emulsifier-induced intestinal
145 inflammation and metabolic deregulation (Chassaing et al., 2017b), mice colonized by AIEC
146 amidst the ASF community are susceptible to emulsifier-induced low-grade inflammation and its
147 metabolic consequences.
148
149 *AIEC colonization results in alterations in microbiota composition upon emulsifier treatment*
150 We envisaged that emulsifiers might have led to inflammation in ASF/AIEC mice *via*
151 promoting increased AIEC abundance and/or more general alteration in microbiota composition
152 and/or activity. To investigate these possibilities, we first examined the impact of emulsifiers on
153 gut microbiota composition of AIEC/ASF mice *via* 16S rRNA gene sequencing. While we
154 previously reported that ASF mice are fully protected against emulsifiers-induced alterations in
155 microbiota composition (Chassaing et al., 2017b), principal coordinate analysis of the
156 unweighted Unifrac distance revealed clear alteration in the microbiota composition of P80-
157 treated AIEC/ASF mice at day 56 compared to their water-treated counterpart (**Figure 2A-C**,
158 Permanova p-value=0.015). This alteration in microbiota composition was not driven by an
159 alteration in the relative abundance of AIEC (**Figure 2D**, based on 16S data), but rather by
160 changes in levels of ASF species with, for example, a complete loss of the Clostridiaceae family
161 (ASF 356 and/or ASF 502 (Gomes-Neto et al., 2017)) in P80-treated mice **(Figure S2A)**. In
162 contrast, CMC administration did not result in a clear overall difference in microbiota of
163 AIEC/ASF mice but was associated with subtle alterations such as an increase in members of the
164 Clostridiaceae family (**Figure S2A**, ASF 356 and/or ASF 502 (Gomes-Neto et al., 2017)) and a

tendency toward a decrease in *Parabacteroides* genus (**Figure S2B**, ASF 519 (Gomes-Neto et al., 2017)). These results are in accord with our previous studies using an *in vitro* microbiota system that suggested that P80 directly alters microbiota composition while CMC directly impacts microbiota gene expression (Chassaing et al., 2017b).

We next examined the extent to which CMC and P80 functionally impacted ability of microbiota to promote intestinal inflammation. One important mediator of host-bacterial interactions is bacterial flagella, which confers motility and whose major component flagellin directly activates host pro-inflammatory gene expression *via* TLR5 and NLRC4 (Franchi et al., 2006; Hayashi et al., 2001). Hence, we used TLR5 reporter cells and observed that, in contrast to ASF mice that do not show any alteration in fecal flagellin in presence of emulsifiers (Chassaing et al., 2017b), CMC or P80 consumption by ASF mice colonized by AIEC resulted in higher levels of flagellin (**Figure 2E-F**), while fecal lipopolysaccharide levels were not affected by emulsifier consumption (**Figure 2G-H**). Use of quantitative PCR applied to purified fecal DNA demonstrated that this increase in fecal flagellin was not due to alteration in fecal bacterial density nor fecal AIEC abundance (**Figure 2I-J**). One potential consequence of increased flagella is a greater ability to penetrate the mucus layer resulting in decreased bacterial-epithelial distance (i.e. microbiota encroachment), which is a feature of gut inflammation in IBD and metabolic syndrome (Chassaing et al., 2015b; Chassaing et al., 2014b; Chassaing et al., 2017a; Sevrin et al., 2018). Confocal analysis of Carnoy-fixed colon specimen to measure the distance separating intestinal bacteria from the surface of the epithelium revealed microbiota encroachment in ASF/AIEC mice that had consumed CMC or P80 (**Figure 3A-D**). In light of these results, we measured intestinal expression of mucin-2 as well as lectin-like protein ZG16

(zymogen granulae protein 16), an abundant mucus protein that contributes to maintenance of bacteria-epithelial distance (Bergstrom JH, 2016, PNAS) and Ly6/PLAUR domain containing 8 (Lypd8), which prevents flagellated microbiota to invade the colonic epithelia. We found that expression of both ZG16 and Lypd8 was increased in CMC-treated ASF/AIEC mice compared to control mice **(Figure S1I-J)**, while expression of mucin-2 was unchanged **(Figure S1H)**. These results suggest that the host responses to repel encroaching bacteria remain functional and are consistent with the notion that promotion of encroachment by emulsifiers might reflect impacts on microbiota. To further understand how CMC and P80 impacted microbiota-epithelial interactions, we utilized laser capture microdissection, which we recently developed as a means to identify inner mucus microbiota (Chassaing and Gewirtz, 2019). This approach indicated that in ASF/AIEC mice, irrespective of emulsifier treatment, a striking majority of the inner mucus bacteria were proteobacteria, specifically AIEC strain LF82 since the ASF community originally lacks Proteobacteria (63.2-82.9%, **Figure 3E**). While neither CMC or P80 markedly impacted relative microbiota composition of inner mucus (**Figure S2C**), the high abundance of AIEC close to the epithelium suggests impacts of emulsifiers on this bacterium might play a key role in mediating impacts of these compounds on the intestine.

AIEC, by itself, is sufficient to make mice prone to detrimental effects of emulsifiers

To investigate the extent to which the impact of CMC and P80 on ASF/AIEC was mediated by AIEC alone or reflected that AIEC can have a long lasting impact on microbiota composition (Bretin et al., 2018; Chassaing et al., 2014a), we mono-colonized germ-free mice with the AIEC reference strain LF82 and subsequently subjected these mice to emulsifier treatment. As presented in **Figure 4**, AIEC by itself made mice prone to pro-inflammatory

impacts of CMC and P80, as reflected by colon weight, colon length and slight increase in spleen weight (**Figure 4A-G**). Moreover, histological scoring of colon specimens indicated significantly increased inflammation in CMC- and P80-treated animals compared to control mice (**Figure 4H and S2D**). Such indices of low-grade inflammation correlated with mild increases in adiposity, although impacts on overall weight was not observed (**Figure 4I-J**). Analogous to observation in ASF mice, combination of all these morphological and molecular measurments into principal coordinate analysis using the Bray-Crutis distance demonstrated a clear and significant clustering of CMC- and P80-treated animals compared with control AIEC monocolonized animals (**Figure S2E**).

We next investigated the intestinal behavior of AIEC LF82 bacteria in response to CMC and P80 exposure. Use of quantitative PCR to quantitate fecal levels of AIEC indicated that absolute AIEC abundance was not impacted by CMC or P80 (**Figure 4K**). However, confocal analysis of Carnoy-fixed colon specimen to measure the distance separating AIEC LF82 bacteria from the surface of the epithelium revealed bacterial encroachment in AIEC mono-colonized mice that had consumed CMC or P80 (**Figure 4L**), suggesting that emulsifier-induced alterations in AIEC gene expression promoted an encroaching phenotype. In any case, collectively, these results indicate that AIEC is sufficient to make mice prone to detrimental impacts of CMC and P80, with the observation that such effects are more pronounced when additional microbial species, such as ASF members, are present.

We next examined if AIEC, by itself, would confer proneness to developing colitis upon emulsifier treatment in $IL10^{-/-}$, which are highly susceptible to developing this disorder in conventional condition but not under germ-free condition (Kuhn et al., 1993; Sellon et al., 1998).

Germ-free IL10$^{-/-}$ mice were mono-colonized with AIEC reference strain LF82 and subsequently administered CMC or P80. Most (80%) of the AIEC-colonized IL-10$^{-/-}$ mice died within 40 days of P80 treatment with marked signs of gut inflammation including slight increase in spleen weight and colon shortening (**Figure 5A-F**). Such severe illness was not seen in CMC-treated mice, rather, such mice displayed evidence of mild inflammation including colon shortening amidst an increased colon weight (**Figure 5A-F**), further illustrating the different impact of CMC and P80 on the host-microbiota relationship, as previously reported (Chassaing et al., 2017b). Analysis of colon expression of CXCL-1, IL1-β, TNF-α by q-RT-PCR supported the notion that AIEC-monoassociated IL10$^{-/-}$ mice were prone to emulsifier-induced gut inflammation (**Figure 5G-I)**, while expression of IL-6 and IL-22 was unchanged **(Figure S3A-B)**. Combinatorily assessing these morphological and molecular measurements *via* principal coordinate analysis of Bray-Crutis distance revealed a clear and significant clustering of CMC- and P80-treated animals compared with control AIEC monocolonized IL10$^{-/-}$ mice (**Figure S3C**). In accord with previous work reporting that high levels of TNFα and IL-1β promote cachexia, gut inflammation in IL-10$^{-/-}$ mice did not result in metabolic syndrome (**Figure 5J-K**).

Another consequence of the inflammation promoted by CMC and P80 is increased proneness to colitis-associated cancer, which was modeled by an AOM injection and repeated exposures to DSS (Viennois et al., 2017). Hence, we examined if mice mono-colonized with AIEC LF82 and concomitantly treated with emulsifiers would exhibit increased carcinogenesis upon AOM/DSS treatment, as schematized in **Figure S1B**. As presented **figure 5L-M**, CMC consumption, but not P80, significantly increased the total tumor count and total tumor area in AIEC mono-colonized mice and enhanced associated intestinal inflammation (**Figure S3D-I**).

Such increased tumor burden suggested the possibility of increased cell proliferation in CMC-treated mice. In accord with this possibility, analysis of proliferation of colonic epithelial cells by Ki67 staining revealed that the consumption of emulsifier by itself (i.e., no AOM/DSS) increased cell proliferation compared with AIEC-mono-colonized water-treated control group (**Figure S4**). AOM/DSS treatment increased the number of Ki67-positive cells in all groups of mice, but the proliferation level remained significantly higher in AOM/DSS-treated mice that had consumed CMC, in accordance with the increased tumor burden observed in this group (**Figure S4**), while P80 exposure did not impacted epithelial cells proliferation. To further address the role of cell turnover in AIEC/emulsifier promotion of colonic carcinogenesis, TUNEL-based quantification of apoptosis in colonic sections was performed. Analogous to our results for cell proliferation, we observed that consumption of emulsifiers by itself (i.e., no AOM/DSS) increased the basal level of TUNEL+ cells in AIEC mono-colonized mice (**Figure S5**). Moreover, this difference between water- and emulsifier-consuming groups was further increased in response to AOM/DSS treatment **(Figure S5)**, indicating that AIEC/emulsifier combination is sufficient to upregulates both apoptosis/proliferation in the intestinal epithelium, resulting in increased cell turnover that can promote tumorigenesis.

Altogether, these data suggest that AIEC bacteria are sufficient to confer proneness to emulsifier-induced intestinal inflammation in WT and genetically susceptible hosts. Such inflammation is sufficient to promote detrimental phenotypes of such inflammation, which are influenced by host genetics and numerous other environmental factors. Moreover, the various models used above further exemplify that CMC and P80 alter the host/microbiota homeostasis through both shared and unique mechanisms.

Dietary emulsifiers increase adherent-invasive Escherichia coli *pathogenic potential through transcriptome modulation*

The results described above suggests that understanding direct impacts of emulsifiers on AIEC might elucidate mechanisms underlying detrimental impacts of these compounds. Hence, we examined impacts of CMC and P80 on AIEC *in vitro*. We first investigated the impact of emulsifier exposure on the defining features of AIEC, namely ability to adhere to and invade intestinal epithelial cells. Only subtle inhibitiory effects on AIEC growth *in vitro* were observed for both CMC and P80 (**Figure S6A-B**), which aligns with our *in vivo* observations that fecal AIEC density is not impacted by emulsifiers exposure. However, we observed that both CMC and P80 increased AIEC adhesion to Int-407 intestinal epithelial cells in a dose dependent manner (**Figure 6A**), while invasion ability was not affected (**Figure 6B**). We next broadly examined the impact of CMC and P80 on AIEC gene expression *via* RNA-Seq approach. CMC dramatically impacted the AIEC LF82 transcriptome in a concentration-dependent manner, as shown in the volcano plots **Figure 6C**. CMC impacted expression of both chromosomal and plasmid gene expression **(Figure S6C-D)**. In contrast, this approach indicated that P80 had only a modest impact on AIEC gene expression. Use of Principal coordinate analysis to visualize these transcriptomes confirmed that CMC induced a strong concentration-dependent alteration in the AIEC transcriptome, while P80 had a subtler, albeit significant, effect (**Figure S7A-B**). Bacterial genes impacted by emulsifier exposure included virulence factors and genes involved in numerous processes, including LPS biosynthesis, DNA replication and transcription (**Figure S7C-G**). For example, expression of *diaA*, which encodes a DnaA initiator-associating protein,

was significantly induced by both CMC and P80 in a dose dependent manner (**Figure S7F**), indicating a broad impact of emulsifier on AIEC replication and fitness (Keyamura et al., 2007). Among numerous virulence factors expressed by AIEC bacteria, flagella (composed by the major sub-unit flagellin FliC and regulated by the FlhDC master regulator), type 1 pili (composed by the major sub-unit FimA) and long polar fimbriae (composed by the major sub-unit LpfA) are known to play central role in bacterial motility, adhesion, and Peyer's patches targeting, respectively (for review, (Palmela et al., 2018). Expression of these virulence factors was significantly increased by CMC in a dose dependent manner (**Figure 6D**), while the effect of P80 seems minimal in regulating AIEC virulence gene expression. Additionally, other genes encoding known AIEC virulence factors were also significantly impacted by emulsifier exposure, as presented in the heatmap **figure S7C**, where CMC induced the expression of numerous known AIEC virulence factors, while P80 had an effect on type VI secretion system. Hence, CMC, and to a much lesser extent, P80, can be directly sensed by AIEC bacteria, leading to alteration in bacterial transcriptome and increases in the expression of numerous virulence factors.

Flagella contributes to AIEC's mediation of emulsifier-induced inflammation

In accord with its impacts on AIEC gene expression, CMC significantly increased flagella-mediated AIEC motility (**Figure 6E**), while P80 did not impact such phenotype. In light of the potential role of flagella/motility in mediating AIEC's promotion of inflammation and mucus penetration (Carvalho et al., 2012; Chassaing et al., 2014a; Sevrin et al., 2018), we next examined if flagellin was necessary for AIEC to confer proneness to emulsifier-induced inflammation. Germ-free WT mice were mono-colonized with AIEC LF82-Δ*fliC* isogenic

mutant and subsequently subjected to emulsifier treatment. Mice monoassociated with aflagellate AIEC exhibited only modest evidence of intestinal inflammation in response to CMC, which was not associated with indices of metabolic syndrome, while P80 wholly lacked impacts in such mice (**Figure 7 and S8**). Moreover, in these LF82-Δ*fliC* mono-colonized mice, the proliferative status of the epithelium was normalized in P80-treated group while the apoptosis activity was normalized in both CMC- and P80-treated group, suggesting a key role played by AIEC flagella in altering the intestinal epithelial cell turnover following emulsifier consumption (**Figure S4 and S5**). Hence, the ability of emulsifiers to increase AIEC's promotion of intestinal inflammation appear to be mediated, in part, by flagella.

DISCUSSION

The intestinal microbiota plays a critical role in mediating the impacts of diet composition upon health (Zmora et al., 2019). The best understood example of this notion is the catabolism of complex carbohydrates by gut bacteria into short-chain fatty acids, which aids energy harvest and has a variety of beneficial impacts upon intestinal health. Moreover, the ability of microbiota composition to broadly predict post-prandial glycemic control in response to a variety of foods underscores the role of specific bacterial taxa in mediating how diet impacts the host (Zeevi et al., 2015). Microbiota is also a key mediator of some of the detrimental impacts that some diets can have on their host. The example germane to this present study is our observation that mice administered 2 common synthetic dietary emulsifiers, CMC and P80, develop gut inflammation that can promote a range of disease states including colitis, metabolic syndrome, and cancer (Chassaing et al., 2015b; Viennois et al., 2017). Such emulsifier-induced inflammation is mediated by microbiota in the sense that it correlates with changes in microbiota composition and localization, and that emulsifiers lack discernable impacts in germ-free mice. Emulsifiers also lack impact in ASF mice, which have a very limited microbiota (Chassaing et al., 2017b), thus suggesting that CMC and P80 disturb the complex inter-relationship between the intestine and the diverse microbial ecosystem it normally harbors, while how such disturbance occur remained unclear. Our findings herein that emulsifiers can directly elicit virulence gene expression and encroachment within the inner mucus inner by pathobiont *E. coli* in a way that is sufficient to make mice prone to detrimental impacts of these compounds help fill this gap of knowledge.

The observation that, in contrast to ASF mice, mice carrying only AIEC or carrying AIEC amidst the other ASF species display emulsifier-induced inflammation leads us to

conclude that the presence of AIEC is sufficient to mediate the detrimental impacts of CMC and P80. While it is more difficult to make firm conclusions regarding how the presence of AIEC makes mice prone to emulsifiers, the ability of these compounds to directly elicit AIEC virulence gene expression *in vitro* suggests a plausible mechanism. Specifically, we hypothesize that, *in vivo*, consumption of CMC and P80, which are non-absorbed, results in their direct interaction with AIEC, increasing expression of genes that facilitate its penetration of the mucus layer and adherence to epithelial cells, resulting in activation of host pro-inflammatory signaling. Hence, we propose that carriage of AIEC may be one specific determinant of the extent to which an individual will be prone to inflammation upon consumption of emulsifiers.

Studies of basic microbial pathogenesis in classic pathogens such as *Salmonella* and Enterohemorragic *E. coli* have revealed complex mechanisms of sensing the environment allowing robust and rapid induction virulence gene expression under select conditions (Duprey et al., 2014; Fang et al., 2016; Jubelin et al., 2018). That AIEC is known to have somewhat analogous sensing machinery (Chassaing and Darfeuille-Michaud, 2013; Chassaing et al., 2013; Chassaing et al., 2011a; Rolhion et al., 2007; Sevrin et al., 2018; Vazeille et al., 2016) suggests that emulsifiers might impact bacterial surfaces due to their detergent properties. Specifically, it suggests the possibility that these compounds may alter AIEC permeability to select molecules, thus altering AIEC periplasm homeostasis, known to play a central role in the regulation of virulence gene expression by AIEC bacteria (Chassaing and Darfeuille-Michaud, 2013; Chassaing et al., 2015a; Rolhion et al., 2007). Such a mechanism offers a potential explanation as to why CMC and P80 might have somewhat similar but yet also distinct impacts on AIEC gene expression, in that these chemically distinct detergents would likely impact permeability in

unique ways. Such a mechanism could also potentially explain the seemingly unusual concentration-dependent effect of P80, in that a low concentration of P80 might permit impact AIEC permeability to specific molecules while higher concentration may also increase permeability to other molecules with countering effect. In any event, analogous dose-dependence of P80 was previously observed *in vivo* (Chassaing et al., 2015b; Chassaing et al., 2017b).

That CMC had a stronger impact on AIEC virulence gene expression than P80 mimics our work with complex human microbiotas in the simulated human intestinal microbiota ecosystem (SHIME) model, in which CMC had a rapid pronounced impact on microbial gene expression that did not associate with differences in species composition (Chassaing et al., 2017b). Conversely, that P80 altered microbiota composition in the SHIME system mimics our observations herein that, in AIEC/ASF mice, only P80 markedly impacted microbiota composition. While the mechanisms explaining these differential impacts of CMC and P80 are not known, they are also potentially explainable by direct impacts of these compounds on microbial surfaces. Interestingly, the detergent-like properties of emulsifiers were pivotal in leading Rhodes and colleagues, and subsequently ourselves, to hypothesize that these compounds might impact host-microbiota interactions and subsequently gut inflammation (Chassaing et al., 2015b; Roberts et al., 2010; Roberts et al., 2013). However, this hypothesis was based on the notion that emulsifiers might impact the functional properties of mucus. While this possibility remains under consideration, our attempts to generate data in support of it have not yet been successful. Rather, our results to date suggest that the impact of emulsifiers on bacteria themselves are sufficient to explain their detrimental impacts.

Direct impacts of emulsifiers on AIEC results in changes in expression of hundreds of genes, in which many of the upregulated genes are putative virulence factors. While we presume that many of these might have potentially important roles in promoting inflammation, that an AIEC flagellar mutant conferred only slight proneness to emulsifier-induced inflammation supports a central role for flagella in mediating impacts of these compounds. Such a role may reflect a role for flagella in mediating mucus penetration, adherence, or activation of innate immune signaling *via* TLR5 or the NLRC4 inflammasome. Future experimentation will be needed to distinguish these possibilities and determine the relative importance of numerous other genes induced by emulsifiers.

CONCLUSION

We demonstrated here that dietary emuslsifier upregulate AIEC virulence gene expression, promoting intestinal inflammation. Moreover, this study further highlights specificities of CMC and P80 effects on pathobionts, suggesting a synergistic detrimental effects of emulsifiers when present in combinations, as it is often the case in processed foods. While determining the importance of emulsifier impacts upon AIEC amidst a complex microbiota remains an important challenge for future studies, we presume that multiple emulsifier-responsive bacteria might be present. Hence, we submit that the extent to which non-absorbed food additives can act directly upon select microbial taxa may prove to be an important consideration in predicting detrimental impacts of food additives (Viennois et al., 2019). Moreover, these findings further support the need for microbiota-based dietary intervention in the management of chronic gut inflammation, in which individuals carrying specific microbiota members will benefit from targeted dietary recommendations.

ACKNOWLEDGEMENTS

This work was supported by an Innovator Award from the Kenneth Rainin Foundation. Moreover, E.V. is a recipient of the Career Development Award from the CCF and an Individual Fellowship Marie Sklodowska-Curie grant from the European Commission Research Executive Agency. B.C. is supported by a Starting Grant from the European Research Council, a Chaire d'Excellence from Paris University and a Career Development Award from the Crohn's and Colitis Foundation (CCF). A.T.G. is supported by NIH grant DK099071 and DK083890. Funders had no role in the design of the study and data collection, analysis and interpretation, nor in manuscript writing. We thank the Hist'IM and Imag'IC platforms (INSERM U1016, Paris, France) for their help.

This work is dedicated to the memory of Arlette Darfeuille-Michaud who pioneered the identification and characterization of AIEC bacteria. In loving memory.

AUTHOR CONTRIBUTIONS

BC obtained funding and conceived and supervised the study. EV, AB, CD and BC performed lab work, analyzed the data, performed statistical analyses, and wrote the manuscript. EV, PED, ACM, NB, ATG and BC analyzed the data and wrote the manuscript. All authors approved the final version of the manuscript.

DECLARATION ON INTEREST

The authors declare that they have no competing interests.

448 **FIGURE LEGENDS**

449 **Figure 1: Colonization by adherent-invasive *Escherichia coli* bacteria is sufficient to**
450 **promote detrimental effects of emulsifiers in normally protected ASF mice.** Six-week-old
451 ASF C57BL/6 mice were colonized with AIEC reference strain LF82 and subsequently exposed
452 to CMC or P80 diluted in drinking water (1.0%) for 12 weeks. (**A**) Colon weight, (**B**) colon
453 length, (**C**) colon weight / length ratio, (**D**) spleen weight, (**E-G**) fecal Lcn2 at day 0 (**E**), day 28
454 (**F**) and day 56 (**G**). Colonic mRNA levels of IL1-β (**H**) and IL10 (**I**). (**J**) colonic histological
455 score, (**K**) final body weight, (**L**) fat pad weight and (**M**) 5hr fasting blood glucose
456 concentration. Data are the means +/- S.E.M (*N*=4-5). *P < .05 compared to water-treated group,
457 determined by a one-way analysis of variance corrected for multiple comparisons with a
458 Bonferroni post-test.

459

460 **Figure 2: Colonization of ASF mice by adherent-invasive *Escherichia coli* bacteria is**
461 **sufficient to induce emulsifier-mediated alterations in microbiota.** Six-week-old ASF
462 C57BL/6 mice were colonized with AIEC reference strain LF82 and subsequently exposed to
463 CMC or P80 diluted in drinking water (1.0%) for 12 weeks. Fecal DNA was extracted and
464 microbiota composition analyzed by 16S rRNA gene sequencing. (**A-C**) Principal coordinate
465 analysis of the unweighted Unifrac distance at day 0 (**A**), day 28 (**B**) and day 56 (**C**). (**D**)
466 Relative abundance of the Enterobacteriaceae family in the fecal microbiota. (**E-F**) Fecal FliC
467 levels at day 0 (**E**) and day 56 (**F**). (**G-H**) Fecal LPS levels at day 0 (**G**) and day 56 (**H**). (**I-J**)
468 Fecal bacterial density (**I**) and relative abundance of AIEC LF82 bacteria at day 56 (**J**). Data are
469 the means +/- S.E.M (*N*=4-5). For clustering analyzing on principal coordinate plots, categories
470 were compared and statistical significance of clustering were determined using Permanova

method. *P < .05 compared to water-treated group, determined by a one-way analysis of variance corrected for multiple comparisons with a Bonferroni post-test.

Figure 3: Colonization by adherent-invasive *Escherichia coli* bacteria is sufficient to induce microbiota encroachment in normally protected ASF mice. Six-week-old ASF C57BL/6 mice were colonized with AIEC reference strain LF82 and subsequently exposed to CMC or P80 diluted in drinking water (1.0%) for 12 weeks. (**A-C**) Confocal microscopy analysis of microbiota localization: Muc2 (green), actin (purple), bacteria (red) and DNA (blue) of water- (**A**), CMC- (**B**) and P80- (**C**) treated mice. Bar = 20 μm. (**D**) Distances of the closest bacteria to intestinal epithelial cells (IEC) per condition over three high-powered fields per mouse. (**E**) Laser capture micro-dissection of inner mucus layer was performed in order to collect mucus-associated microbiota. Fecal and mucus-associated microbiota composition was analyzed by 16S rRNA gene Illumina sequencing. Taxa summarization performed at the phylum level is represented. Data are the means +/- S.E.M (*N*=4-5). *P < .05 compared to water-treated group, determined by a one-way analysis of variance corrected for multiple comparisons with a Bonferroni post-test.

Figure 4: Mono-colonization by adherent-invasive *Escherichia coli* bacteria is sufficient to drive detrimental effects of emulsifiers in WT mice. Six-week-old germ-free C57BL/6 mice were mono-colonized with AIEC reference strain LF82 and subsequently exposed to CMC or P80 diluted in drinking water (1.0%) for 12 weeks. (**A**) Colon weight, (**B**) colon length, (**C**) colon weight / length ratio, (**D**) spleen weight, (**E-G**) fecal Lcn2 at day 0 (**E**), day 28 (**F**) and day 56 (**G**), (**H**) colonic histological score, (**I**) final body weight, (**J**) fat pad weight, (**K**) relative

494 abundance of AIEC LF82 bacteria at day 56 and (**L**) distances of the closest AIEC bacteria to
495 intestinal epithelial cells (IEC) per condition over three high-powered fields per mouse. Data are
496 the means +/- S.E.M (*N*=4-5). *P < .05 compared to water-treated group, determined by a one-
497 way analysis of variance corrected for multiple comparisons with a Bonferroni post-test.
498
499 **Figure 5: Mono-colonization by adherent-invasive *Escherichia coli* bacteria is sufficient to**
500 **drive detrimental effects of emulsifiers in IL10$^{-/-}$ mice and promotion of colon cancer in WT**
501 **mice.** (**A-K**) Six-week-old germ-free (GF) IL10$^{-/-}$ C57BL/6 mice were colonized with AIEC
502 reference strain LF82 and subsequently exposed to CMC or P80 diluted in drinking water (1.0%)
503 for 12 weeks. (**A**) Survival curve, (**B**) colon weight, (**C**) colon length, (**D**) colon weight / length
504 ratio, (**E**) spleen weight, (**F**) caecum weight, (**G**) final body weight and (**H**) fat pad weight. (**I-K**)
505 Colonic mRNA levels of Cxcl1 (**I**), IL1-β (**J**) and TNF-α (**K**). (**L-M**) Six-week-old germ-free
506 C57BL/6 mice were mono-colonized with AIEC reference strain LF82 and subsequently
507 exposed to CMC or P80 diluted in drinking water (1.0%) for 12 weeks in combination with an
508 AOM/DSS protocol. (**L**) Number of tumors per mouse and (**M**) total surface or tumor area in
509 mm^2. Data are the means +/- S.E.M (*N*=5). *P < .05 compared to water-treated group,
510 determined by a one-way analysis of variance corrected for multiple comparisons with a
511 Bonferroni post-test.
512
513 **Figure 6: Dietary emulsifiers increase adherent-invasive *Escherichia coli* pathogenic**
514 **potential through transcriptome modulation.** Adhesion (**A**) and invasion (**B**) abilities of AIEC
515 LF82 grown *in vitro* with various concentration of CMC and P80 with intestinal epithelial cells
516 (I-407). (**C**) AIEC reference strain LF82 was grown *in vitro* with various concentration of CMC

517 and P80, mRNAs extracted and subjected to RNA-Seq analysis. Chromosomic genes were
518 visualized on a volcano plot as follow: Up/left: water-treated versus CMC- 1.0000%-treated;
519 up/middle: water-treated versus CMC- 0.2500%-treated; up/right: water-treated versus CMC-
520 0.0625%-treated; bottom/left: water-treated versus P80- 1.0000%-treated; bottom /middle: water-
521 treated versus P80- 0.2500%-treated; bottom /right: water-treated versus P80- 0.0625%-treated.
522 For each chromosomic gene, the difference in abundance between the two groups is indicated in
523 log2 fold change on *x*-axis (with positive values corresponding to an increase in emulsifier-
524 treated group compare to water-treated group, and negative values corresponding to a decrease in
525 emulsifier-treated group compare to water-treated group), and significance between the two
526 groups is indicated by -log10 *p*-value on the *y*-axis. Red dots correspond to chromosomic genes
527 with a *p*-value <0.05 between emulsifier-treated and water-treated groups. Orange dots
528 correspond to chromosomic genes with at least a 2-fold decreased or increased abundance in
529 emulsifier-treated group compare to water-treated group. Green dots correspond to chromosomic
530 genes with at least a 2-fold decreased or increased abundance in emulsifier-treated group
531 compare to water-treated group and with a *p*-value <0.05. (**D**) AIEC reference strain LF82 was
532 grown *in vitro* with various concentration of CMC and P80, mRNAs extracted and subjected to
533 q-RT-PCR analysis of *fliC*, *flhDC*, *fimA* and *lpfA* gene expression. (**E**) Motility assay of AIEC
534 reference strain LF82 grown *in vitro* with various CMC or P80 (1%). Bacteria were washed
535 before inoculation of 0.3% agar medium and motility was assessed quantitatively 15 hours post
536 inoculation by examining the circular swimming motion formed by the growing motile bacterial
537 cells. Data are the means +/- S.E.M (*N*=2-6). *P < .05 compared to water-treated group,
538 determined by a one-way analysis of variance corrected for multiple comparisons with a
539 Bonferroni post-test.

Figure 7: Bacterial flagellin contributes to AIEC-mediated emulsifier detrimental effects. Six-week-old germ-free C57BL/6 mice were mono-colonized with AIEC LF82-Δ*fliC* mutant and subsequently exposed to CMC or P80 diluted in drinking water (1.0%) for 12 weeks. (**A**) Colon weight, (**B**) colon length, (**C**) colon weight / length ratio, (**D**) spleen weight, (**E-G**) fecal Lcn2 at day 0 (**E**), day 28 (**F**) and day 56 (**G**), (**H**) colonic histological score, (**I**) final body weight (**J**) fat pad weight and (**K**) relative abundance of AIEC LF82 bacteria at day 56. Data are the means +/- S.E.M (N=3). *P < .05 compared to water-treated group, determined by a one-way analysis of variance corrected for multiple comparisons with a Bonferroni post-test.

549 **STAR METHODS**

550 **KEY RESSOURCE TABLE AVAILABILITY**

REAGENT or RESOURCE	SOURCE	IDENTIFIER
Antibodies		
Anti-Mucin 2	Santa Cruz Biotechnology	Cat. # sc-15334; RRID: AB_2146667
Alexa Fluor 488 Goat Anti-Rabbit IgG	Invitrogen	Cat.# A11008; RRID: AB_143165
Chemicals, Peptides, and Recombinant Proteins		
Sodium carboxymethylcellulose	Sigma-Aldrich	419311
Polysorbate-80	Sigma-Aldrich	P1754
Phalloidin–Tetramethylrhodamine B isothiocyanate	Sigma-Aldrich	Cat.# P1951-.1MG
Rodent chow	LabDiet	Cat. # 5001
Luria Broth	BD	Cat. # BD 244620
Azoxymethane	Sigma-Aldrich	Cat. # A5486
Dextran sulfate sodium salt, colitis grade (36,000 - 50,000)	MP Biomedical	Cat. # SKU 02160110-CF
Critical Commercial Assays		
One-Step RT–PCR Kit with SYBR Green	Qiagen	Cat. # 204154
Duoset murine Lcn-2 ELISA kit	R&D Systems	Cat. # DY1857
In Situ Cell Death Detection Kit	Roche Diagnostics	Cat. # 11684795910
Deposited Data		
16S sequencing: unprocessed sequencing data	This paper	CRA003162
RNA-Seq: unprocessed sequencing data	This paper	CRA003155
Experimental Models: Organisms/Strains		
Mice: C57BL/6	Taconic Inc	Cat. # C57BL/6NTac
Mice: C57BL/6 IL10-/-	Taconic Inc	Cat. # GF-16006
Oligonucleotides		
See Table S1	This study	N/A
Software and Algorithms		
GraphPad Prism	GraphPad Software	Version 8

551

552

553

554

RESOURCE AVAILABILITY

Lead Contact

Further information and requests for resources and reagents should be directed to and will be fulfilled by the Lead Contact, Benoit Chassaing (benoit.chassaing@inserm.fr).

Materials Availability

This study did not generate new unique reagents

Data and Code Availability

Unprocessed sequencing data are deposited in the Genome Sequence Archive (GSA) in BIG Data Center , Beijing Institute of Genomics, Chinese Academy of Sciences, under accession numbers CRA003155 and CRA003162, publicly accessible at https://bigd.big.ac.cn/gsa.

EXPERIMENTAL MODEL AND SUBJECT DETAILS

Mice

C57BL/6 mice (C57BL/6NTac) were maintained in gnotobiotic conditions in a germ-free (GF) or Altered Schaedler flora state (ASF, containing the 8 bacteria *Clostridium sp.* (ASF356), *Lactobacillus intestinalis* (ASF360), *Lactobacillus murinus* (ASF361), *Mucispirillum shaedleri* (ASF457), *Eubacterium plexicaudatum* (ASF492), *Firmicutes bacterium* (ASF500), *Clostridium sp.* (ASF502) and *Parabacteroides sp.* (ASF519)) in a Park Bioservices isolator as previously described (Chassaing et al., 2015b). Germ-free C57BL/6 IL10-/- male mice (C57BL/6NTac-*Il10*^{em8Tac}; Taconic model GF-16006) were maintained in isolated ventilated cages Isocages (Techniplast, West Chester, PA, USA) (Hecht et al., 2014). All mice were bred and housed at Georgia State University (Atlanta, GA, USA) under institutionally-approved protocols (IACUC # A17047 and A18006). Mice were fed autoclaved LabDiet rodent chow # 5021. ASF mice were

established by colonizing WT C57BL/6 GF mice with the complete Altered Schaedler flora (8 strains) using feces purchased from ASF Taconic Biosciences Inc. and resuspended in drinking water, as previously described (Chassaing and Gewirtz, 2018). Mice used in this study were 4-5 weeks old.

Materials

Sodium carboxymethylcellulose (CMC, average MW ~250,000) and Polysorbate-80 (P80) were purchased from Sigma (Sigma, St. Louis, MO).

METHOD DETAILS

Colonization with Adherent Invasive *Escherichia coli* strain LF82

For mono-colonization of germ-free mice and colonization of ASF mice with Adherent Invasive *Escherichia coli* (AIEC), reference strain LF82 and LF82-Δ*fliC* mutant were grown overnight in 200 mL of LB at 37C without agitation. Bacterial suspensions with an OD_{620nm} of 2.0 were placed in the water bottles of germ-free or ASF C57Bl/6 mice placed in isolated ventilated caging system (Isocage) that prevents exogenous bacterial contamination. One week later, water solution was put back and supplemented with CMC or P80 (1.0%) (**Figure S1**). After 12 weeks, mice were euthanized and their organs were collected for downstream analysis.

Emulsifier agent treatment

Mice were exposed to CMC or P80 diluted in the drinking water (1.0%). The same water (reverse-osmosis treated Atlanta city water) was used for the water-treated (control) group. Emulsifier solutions were autoclaved and changed every week. Fresh feces were collected every

other week for downstream analysis. After 3 months of emulsifier treatment, body weight was measured and blood was collected by retrobulbar intraorbital capillary plexus. Hemolysis-free serum was generated by centrifugation of blood using serum separator tubes (Becton Dickinson, Franklin Lakes, NJ). Mice were then euthanized and adipose weight, spleen weight, caecum weight, colon length, and colon weight were measure. Organs were collected for downstream analysis.

Fasting blood glucose measurement

Mice were placed in a clean cage and fasted for 5h. Blood glucose concentration was then determined using a Nova Max Plus Glucose Meter and expressed in mg/dL.

Colitis-associated cancer model

Colitis-associated cancer (CAC) was induced as previously described with some modifications (Greten et al., 2004; Viennois et al., 2017). As schematized in **Figure S1**, after mono-association with AIEC reference strain LF82 and 4 weeks of emulsifier administration, mice were intraperitoneally injected with AOM (10 mg/kg body weight) (Sigma-Aldrich, St. Louis, MO) diluted in PBS and maintained on autoclaved chow diet and water or emulsifier-supplemented water for 5 days. Mice were then subjected to two cycles of DSS treatment (MP Biomedicals, Solon, OH, USA), in which each cycle consisted of 2.5% DSS for 7 days followed by a 14-day recovery period with regular water or emulsifier-supplemented water. After treatment, mice were fasted for 5h at which time blood was collected by retrobulbar intraorbital capillary plexus. Hemolysis-free serum was generated by centrifugation of blood using serum separator tubes (Becton Dickinson, Franklin Lakes, NJ). After colitis-associated cancer protocol,

mice were euthanized, and colon length, colon weight, spleen weight and adipose weight were measure. Organs and blood were collected for downstream analysis. Colonic tumors were counted and surface measured using a dissecting microscope. The total area of tumors for each colon was determined.

Adhesion and invasion assay

The bacterial adhesion assay was performed as described previously (Boudeau et al., 1999). Briefly, Intestine-407 cells were seeded in 24-well tissue culture plates with 4 x 10^5 cells per well. Monolayers were then infected at a multiplicity of infection of 10 bacteria per cell in 1 ml of the cell culture medium without antibiotics and with heat-inactivated fetal calf serum (FCS, PAA), using bacteria grown at 37°C in LB with or without CMC or P80 at various concentration (0.0625, 0.2500 and 1.0000) and subsequently washed twice in PBS in order to avoid any direct effect of emulsifier on adhesion and invasion processes. After a 3 h incubation period at 37°C, monolayers were washed three times in phosphate-buffered saline (PBS, pH 7.2). Epithelial cells were then lysed with 1% Triton X-100 (Euromedex) in deionized water. Samples were diluted and plated onto Muller-Hinton agar plates to determine the number of colony-forming units (CFU) corresponding to the total number of cell-associated bacteria (adherent and intracellular bacteria). In order to determine the number of intracellular bacteria, fresh cell culture medium containing 100 $mg.ml^{-1}$ gentamicin was added for 1h to kill extracellular bacteria. Monolayers were then lysed with 1% Triton X-100, and bacteria were quantified as described above.

647

648 **Motility assay**

649 Bacterial strains were grown overnight at 37°C without agitation in LB broth with CMC
650 or P80 at 1.0% concentration, and 2µl portions of the culture were inoculated into the center of
651 0.3% LB agar plates. The plates were then incubated at 37°C, and motility was assessed
652 quantitatively 15 hours post inoculation by examining the circular swimming motion formed by
653 the growing motile bacterial cells.

654

655 **AIEC transcriptomic analysis**

656 Cultures were grown at 37°C in LB with or without CMC or P80 at various concentration
657 (0.0625, 0.2500 and 1.0000). Total mRNAs were extracted from overnight-cultured bacteria and
658 treated with DNase (Roche Diagnostics) to remove any contaminating genomic DNA. After
659 purification, RNA concentration and integrity were determined using Epoch Microplate
660 Spectrophotometer (Bio-Tek, Winooski, VT, USA) and agarose gel electrophoresis, respectively.
661 rRNAs were removed using Ribo-Zero® rRNA Removal Kit (Illumina) and total mRNAs were
662 then prepared for sequencing using Illumina TruSeq RNA kit according to the manufacturer's
663 protocol. Briefly, rRNA-depleted RNAs were fragmented, and converted to cDNA. After end
664 repair and ligation of adapters, mRNA libraries were amplified by PCR and validated using
665 BioAnalyser, according to manufacturer's recommendations. The purified library was then
666 subjected to sequencing using an Illumina NextSeq500 (single end, 75bp) at the Cornell
667 University sequencing core (Ithaca, NY). Sequencing data obtained were analyzed by alignment
668 against LF82 genome (both chromosome and plasmid (Miquel et al., 2010)) using bowtie 2
669 software (Langmead and Salzberg, 2012), and gene expression were compared between

conditions using cufflinks (Trapnell et al., 2012). Data were visualized using principal coordinate analysis of the Euclidean distance, volcano plot created using R software, heatmap representation using Morpheus (Chassaing et al., 2017b). Unprocessed sequencing data are deposited in the Genome Sequence Archive (GSA)46 in BIG Data Center 47, Beijing Institute of Genomics, Chinese Academy of Sciences, under accession number CRA003155, publicly accessible at https://bigd.big.ac.cn/gsa.

Quantification of fecal lipocalin-2 (Lcn-2) by ELISA

For quantification of fecal Lcn-2 by ELISA, frozen fecal samples were reconstituted in PBS containing 0.1% Tween 20 to a final concentration of 100 mg/mL and vortexed for 20 min to get a homogenous fecal suspension (Chassaing et al., 2012). These samples were then centrifuged for 10 min at 14 000 g and 4°C. Clear supernatants were collected and stored at −20°C until analysis. Lcn-2 levels were estimated in the supernatants using Duoset murine Lcn-2 ELISA kit (R&D Systems, Minneapolis, MN, USA) using the colorimetric peroxidase substrate tetramethylbenzidine, and optical density (OD) was read at 450 nm (Versamax microplate reader).

Colonic RNAs extraction and q-RT-PCR analysis

Distal colon was collected during euthanasia and placed in RNAlater. Total RNAs were isolated from colonic tissues using TRIzol (Invitrogen, Carlsbad, CA) according to the manufacturer's instructions and as previously described (Chassaing et al., 2012). Quantitative RT-PCR were performed using the Qiagen kit QuantiFast® SYBR® Green RT-PCR in a CFX96 apparatus (Bio-Rad, Hercules, CA) with specific mouse oligonucleotides (**Table S1**). Gene

693 expression are presented as relative values using the ΔΔCt approach with 36B4 housekeeping
694 gene.
695
696
697 **Ki67 immunohistochemistry**
698 Mouse proximal colon devoid of tumor were fixed in 10%-buffered formalin for 24 h at
699 room temperature and subsequently embedded in paraffin. Tissues were sectioned at 5-μm
700 thickness and deparaffinized. Sections were incubated in sodium citrate buffer and cooked in a
701 pressure cooker for 10 minutes for antigen retrieval. Sections were then blocked with 5% goat
702 serum in TBS followed by one-hour incubation with anti-Ki67 (1:100, Vector Laboratories,
703 Burlingame, CA) at 37º C. After washing with TBS, sections were treated with biotinylated
704 secondary antibodies for 30 minutes at 37°C, and color development was performed using the
705 Vectastain ABC kit (Vector Laboratories). Sections were then counterstained with hematoxylin,
706 dehydrated, and coverslipped. Ki67-positive cells were counted per crypt.
707
708 **Terminal deoxynucleotidyl transferase deoxyuridine triphosphate nick-end labeling**
709 **(TUNEL)**
710 To quantitate the number of apoptotic cells in colonic epithelial cells, mouse proximal
711 colon devoid of tumor were fixed in 10%-buffered formalin for 24 h at room temperature,
712 embedded in paraffin, sectioned at 5-μm thickness, deparaffinized and stained for apoptotic
713 nuclei according to the manufacturer's instructions using the In Situ Cell Death Detection Kit
714 (Roche Diagnostics, Indianapolis, IN). TUNEL-positive cells overlapping with DAPI nuclear
715 staining were counted per crypt.

716

717 **H&E Staining of Colonic Tissue and Histopathologic Analysis**

718 Mouse colons were fixed in 10% buffered formalin for 24 hours at room temperature and
719 then embedded in paraffin. Tissues were sectioned at 5-µm thickness and stained with
720 hematoxylin & eosin (H&E) using standard protocols. Images were acquired using a Lamina
721 (Perkin Elmer) at the Hist'IM platform (INSERM U1016, Paris, France). Histological scoring
722 was blindly determined on each colon as previously described (Chassaing et al., 2012; Katakura
723 et al., 2005). Briefly, each colon was assigned four scores based on the degree of epithelial
724 damage and inflammatory infiltrate in the mucosa, submucosa and muscularis/serosa (Katakura
725 et al., 2005). Each of the four scores was multiplied by a coefficient 1 if the change was focal, 2
726 if it was patchy and 3 if it was diffuse (Chassaing et al., 2012) and the 4 individual scores per
727 colon were added.

728

729 **Immunostaining of mucins and localization of bacteria by FISH**

730 Mucus immunostaining was paired with fluorescent *in situ* hybridization (FISH), as
731 previously described (Johansson and Hansson, 2012), in order to analyze bacteria localization at
732 the surface of the intestinal mucosa (Chassaing et al., 2015b; Chassaing et al., 2014b). Briefly,
733 colonic tissues (proximal colon, 2nd cm from the cecum) containing fecal material were placed
734 in methanol-Carnoy's fixative solution (60% methanol, 30% chloroform, 10% glacial acetic
735 acid) for a minimum of 3 h at room temperature. Tissues were then washed in methanol 2 x 30
736 min, ethanol 2 x 15 min, ethanol/xylene (1:1) 15 min and xylene 2 x 15 min, followed by
737 embedding in Paraffin with a vertical orientation. Five µm sections were performed and dewax
738 by preheating at 60°C for 10 min, followed by xylene 60°C for 10 min, xylene for 10 min and

739 99.5% ethanol for 10 minutes. Hybridization step was performed at 50°C overnight with
740 EUB338 probe (5'-GCTGCCTCCCGTAGGAGT-3', with a 5' labeling using Alexa 647) diluted
741 to a final concentration of 10 µg/mL in hybridization buffer (20 mM Tris–HCl, pH 7.4, 0.9 M
742 NaCl, 0.1% SDS, 20% formamide). After washing 10 min in wash buffer (20 mM Tris–HCl, pH
743 7.4, 0.9 M NaCl) and 3 x 10 min in PBS, PAP pen (Sigma-Aldrich) was used to mark around the
744 section and block solution (5% fetal bovine serum in PBS) was added for 30 min at 4°C. Mucin-
745 2 primary antibody (rabbit H-300, Santa Cruz Biotechnology, Dallas, TX, USA) was diluted
746 1:1500 in block solution and apply overnight at 4°C. After washing 3 x 10 min in PBS, block
747 solution containing anti-rabbit Alexa 488 secondary antibody diluted 1:1500, Phalloidin-
748 Tetramethylrhodamine B isothiocyanate (Sigma-Aldrich) at 1µg/mL and Hoechst 33258 (Sigma-
749 Aldrich) at 10µg/mL was applied to the section for 2h. After washing 3 x 10 min in PBS slides
750 were mounted using Prolong anti-fade mounting media (Life Technologies, Carlsbad, CA,
751 USA). Observations were performed with a Zeiss LSM 700 confocal microscope with software
752 Zen 2011 version 7.1. This software was used to determine the distance between bacteria and
753 epithelial cell monolayer, as well as the mucus thickness.
754
755 **Immunostaining of mucins and localization of AIEC bacteria**
756 Mucus immunostaining was performed as described above. Anti Mucin-2 (from rabbit,
757 Gene Tex, Irvine, CA, United States) anti *Escherichia coli* (from goat Biorad, Hercules, CA,
758 United States)primary antibodies were diluted 1:500 in block solution and apply overnight at
759 4°C. After washing 3 x 10 min in PBS, block solution containing anti-rabbit Alexa 488 and anti-
760 goat Alexa 647 secondary antibodies diluted 1:1500, Phalloidin-Tetramethylrhodamine B
761 isothiocyanate (Sigma-Aldrich) at 1µg/mL and Hoechst 33258 (Sigma-Aldrich) at 10µg/mL was

applied to the section for 2h. After washing 3 x 10 min in PBS slides were mounted using Prolong anti-fade mounting media (Life Technologies, Carlsbad, CA, USA). Image acquisition were performed at the IMAG'IC Platform (INSERM U1016, Paris, France) using a Spinning-Disk IXplore (Olympus). Olyvia software (Olympus) was used to determine the distance between bacteria and epithelial cell monolayer.

Inner mucus microdissection

Microdissection were performed on an Arcturus® Laser Capture Microdissection system, as previously described (Chassaing and Gewirtz, 2019). Inner mucus layers were selected and collected on CapSure™ Macro LCM Caps (Arcturus) using a combination of infrared (IR) capture and ultraviolet (UV) laser cutting. The membrane covering caps were subsequently carefully collected, placed in clean DNA-free 0.5mL tubes, and store in -80°C until DNA extraction.

DNA extraction and 16S rRNA gene amplification from laser capture microdissected mucus

As previously described (Chassaing and Gewirtz, 2019), Qiagen QIAamp DNA Micro Kit were used to isolate DNA from laser-microdissected inner mucus. 30µL of buffer ATL and 20µL of proteinase K were added to the microdissected samples and incubated at 56°C overnight. 50µL of buffer ATL and 100µL of buffer AL were added, sample were mixed by vortexing, and 100µL of ethanol was added followed by a 5 min incubation at room temperature. The sample was next transferred to a QIAamp MinElute column (without the membrane) and centrifuge at 6,000 g for 1 min. The column was washed with 500µL of buffer AW1 and 500µL of buffer AW2 and dried with a 3 min centrifugation at 20,000 g. 20µL of DNA free water

(Mobio) were then applied to the center of the column, incubated at room temperature for 10min, followed by a final centrifugation at 20,000 g for 1min in order to collect eluted DNA. Microbiota analysis was subsequently performed by 16S rRNA gene sequencing using Illumina technology, as described above.

Fecal flagellin and lipopolysaccharide load quantification

Levels of fecal bioactive flagellin and lipopolysaccharide (LPS) were quantified as previously described (Chassaing et al., 2014a) using human embryonic kidney (HEK)-Blue-mTLR5 and HEK-BluemTLR4 cells, respectively (Invivogen, San Diego, CA, USA) (Chassaing et al., 2014a). Fecal material was resuspended in PBS to a final concentration of 100 mg/mL and homogenized for 10 s using a Mini-Beadbeater-24 without the addition of beads to avoid bacteria disruption. Samples were then centrifuged at 8000 g for 2 min and the resulting supernatant was serially diluted and applied on mammalian cells. Purified *E. coli* flagellin and LPS (Sigma-Aldrich) were used for standard curve determination using HEK-Blue-mTLR5 and HEK-Blue-mTLR4 cells, respectively. After 24 h of stimulation, the cell culture supernatant was applied to QUANTI-Blue medium (Invivogen) and the alkaline phosphatase activity was measured at 620 nm after 30 min.

Bacterial RNAs extraction and q-RT-PCR analysis

Cultures were grown at 37°C in LB with or without CMC or P80 at various concentration (0.015625, 0.031250, 0.062500, 0.125000, 0.250000, 0.500000 and 1.000000). Total mRNAs were extracted from overnight-cultured bacteria and treated with DNase (Roche Diagnostics) to remove any contaminating genomic DNA. Total RNAs were amplified by RT-PCR using

specific primers to 16S, *fliC*, *flhDC*, *fimA* and *lpfA* (**Table S1**) on a Biorad CFX96 apparatus (BioRad) using iTaq™ Universal SYBR® Green One-Step Kit (BioRad) with 0.25 µg of total RNA. Amplification of a single expected PCR product was confirmed by electrophoresis on a 2% agarose gel.

Microbiota analysis by 16S rRNA gene sequencing using Illumina technology

16S rRNA gene amplification and sequencing were done using the Illumina MiSeq technology following the protocol of Earth Microbiome Project with their modifications to the MOBIO PowerSoil DNA Isolation Kit procedure for extracting DNA (www.earthmicrobiome.org/emp-standard-protocols) (Caporaso et al., 2012; Gilbert et al., 2010). Bulk DNA was extracted from frozen feces using a PowerSoil-htp kit from MoBio Laboratories (Carlsbad, CA, USA) with mechanical disruption (bead-beating). The 16S rRNA genes, region V4, were PCR amplified from each sample using a composite forward primer and a reverse primer containing a unique 12-base barcode, designed using the Golay error-correcting scheme, which was used to tag PCR products from respective samples (Caporaso et al., 2012). We used the forward primer 515F 5'-*AATGATACGGCGACCACCGAGATCTACACGCT*XXXXXXXXXXXX**TATGGTAATT*GT***G TGYCAGCMGCCGCGGTAA-3': the italicized sequence is the 5' Illumina adapter, the 12 X sequence is the golay barcode, the bold sequence is the primer pad, the italicized and bold sequence is the primer linker and the underlined sequence is the conserved bacterial primer 515F. The reverse primer 806R used was 5'-*CAAGCAGAAGACGGCATACGAGAT***AGTCAGCCAG*CC*** GGACTACNVGGGTWTCTAAT-3': the italicized sequence is the 3' reverse complement sequence of Illumina adapter, the bold

831 sequence is the primer pad, the italicized and bold sequence is the primer linker and the
832 underlined sequence is the conserved bacterial primer 806R. PCR reactions consisted of Hot
833 Master PCR mix (Quantabio, Beverly, MA, USA), 0.2 μM of each primer, 10-100 ng template,
834 and reaction conditions were 3 min at 95°C, followed by 30 cycles of 45 s at 95°C, 60s at 50°C
835 and 90 s at 72°C on a Biorad thermocycler. PCRs products were purified with Ampure magnetic
836 purification beads (Agencourt, Brea, CA, USA), and visualized by gel electrophoresis. Products
837 were then quantified (BIOTEK Fluorescence Spectrophotometer) using Quant-iT PicoGreen
838 dsDNA assay. A master DNA pool was generated from the purified products in equimolar ratios.
839 The pooled products were quantified using Quant-iT PicoGreen dsDNA assay and then
840 sequenced using an Illumina MiSeq sequencer (paired-end reads, 2 x 250 bp) at Cornell
841 University, Ithaca.
842
843 **16S rRNA gene sequence analysis**
844 Forward and reverse Illumina reads were joined using the fastq-join method (Aronesty,
845 2011, 2013), sequences were demultiplexed, quality filtered using Quantitative Insights Into
846 Microbial Ecology (QIIME, version 1.8.0) software package (Caporaso et al., 2010). QIIME
847 default parameters were used for quality filtering (reads truncated at first low-quality base and
848 excluded if: (1) there were more than three consecutive low quality base calls (2), less than 75%
849 of read length was consecutive high quality base calls (3), at least one uncalled base was present
850 (4), more than 1.5 errors were present in the bar code (5), any Phred qualities were below 20, or
851 (6) the length was less than 75 bases). Sequences were assigned to operational taxonomic units
852 (OTUs) using UCLUST algorithm (Edgar, 2010) with a 97% threshold of pairwise identity (with
853 the creation of new clusters with sequences that do not match the reference sequences), and

854 classified taxonomically using the Greengenes reference database 13_8 (McDonald et al., 2012).
855 A single representative sequence for each OTU was aligned and a phylogenetic tree was built
856 using FastTree (Price et al., 2009). The phylogenetic tree was used for computing the
857 unweighted UniFrac distances between samples (Lozupone et al., 2006; Lozupone and Knight,
858 2005), rarefaction were performed and used to compare abundances of OTUs across samples.
859 Principal coordinates analysis (PCoA) plots were used to assess the variation between
860 experimental group (beta diversity). Unprocessed sequencing data are deposited in the Genome
861 Sequence Archive (GSA)46 in BIG Data Center 47, Beijing Institute of Genomics, Chinese
862 Academy of Sciences, under accession number CRA003162, publicly accessible at
863 https://bigd.big.ac.cn/gsa.
864
865 **Bacterial density quantification by 16S rRNA qPCR**
866 Extracted DNAs were diluted 1/10 with sterile DNA-free water and amplified by quantitative
867 PCR using the 16S V4 specific primers 515F 5'-GTGYCAGCMGCCGCGGTAA-3' and 806R
868 5'-GGACTACNVGGGTWTCTAAT-3' or using the using the AIEC LF82 PTM specific
869 primers PTM-F 5'- CCATTCATGCAGCAGCTCTTT -3' and PTM-R 5'-
870 ATCGGACAACATTAGCGGTGT -3' on a LightCycler 480 (Roche) using QuantiFast SYBR®
871 Green PCR Kit (Qiagen). Amplification of a single expected PCR product was confirmed by
872 electrophoresis on a 2% agarose gel, and data are expressed as relative values normalized with
873 feces weight used for DNA extraction.
874
875 **QUANTIFICATION AND STATISTICAL ANALYSIS**
876 Results were expressed as mean ± SEM. Significance was determined using one-way

877 group ANOVA with Bonferroni's multiple comparisons test (GraphPad Prism software, version
878 6.01). Differences were noted as significant *$p \leq 0.05$. For clustering analysis on principal
879 coordinate plots, categories were compared and statistical significance of clustering was
880 determined *via* Permanova.

881 **REFERENCES**

882 Aronesty, E. (2011). Command-line tools for processing biological sequencing data.
883 http://codegooglecom/p/ea-utils.

884 Aronesty, E. (2013). Comparison of Sequencing Utility Programs. The Open Bioinformatics
885 Journal *7*, 1-8.

886 Arthur, J.C., Perez-Chanona, E., Muhlbauer, M., Tomkovich, S., Uronis, J.M., Fan, T.J.,
887 Campbell, B.J., Abujamel, T., Dogan, B., Rogers, A.B.*, et al.* (2012). Intestinal inflammation
888 targets cancer-inducing activity of the microbiota. Science *338*, 120-123.

889 Barnich, N., Bringer, M.A., Claret, L., and Darfeuille-Michaud, A. (2004). Involvement of
890 lipoprotein NlpI in the virulence of adherent invasive Escherichia coli strain LF82 isolated from
891 a patient with Crohn's disease. Infection and immunity *72*, 2484-2493.

892 Barnich, N., Carvalho, F.A., Glasser, A.L., Darcha, C., Jantscheff, P., Allez, M., Peeters, H.,
893 Bommelaer, G., Desreumaux, P., Colombel, J.F.*, et al.* (2007). CEACAM6 acts as a receptor for
894 adherent-invasive E. coli, supporting ileal mucosa colonization in Crohn disease. The Journal of
895 clinical investigation *117*, 1566-1574.

896 Boudeau, J., Glasser, A.L., Masseret, E., Joly, B., and Darfeuille-Michaud, A. (1999). Invasive
897 ability of an Escherichia coli strain isolated from the ileal mucosa of a patient with Crohn's
898 disease. Infection and immunity *67*, 4499-4509.

899 Bretin, A., Lucas, C., Larabi, A., Dalmasso, G., Billard, E., Barnich, N., Bonnet, R., and Nguyen,
900 H.T.T. (2018). AIEC infection triggers modification of gut microbiota composition in genetically
901 predisposed mice, contributing to intestinal inflammation. Sci Rep *8*, 12301.

902 Cani, P.D., Osto, M., Geurts, L., and Everard, A. (2012). Involvement of gut microbiota in the
903 development of low-grade inflammation and type 2 diabetes associated with obesity. Gut
904 Microbes *3*, 279-288.
905 Caporaso, J.G., Kuczynski, J., Stombaugh, J., Bittinger, K., Bushman, F.D., Costello, E.K.,
906 Fierer, N., Pena, A.G., Goodrich, J.K., Gordon, J.I.*, et al.* (2010). QIIME allows analysis of high-
907 throughput community sequencing data. Nat Med *7*, 335-336.
908 Caporaso, J.G., Lauber, C.L., Walters, W.A., Berg-Lyons, D., Huntley, J., Fierer, N., Owens,
909 S.M., Betley, J., Fraser, L., Bauer, M.*, et al.* (2012). Ultra-high-throughput microbial community
910 analysis on the Illumina HiSeq and MiSeq platforms. The ISME journal *6*, 1621-1624.
911 Carvalho, F.A., Koren, O., Goodrich, J.K., Johansson, M.E., Nalbantoglu, I., Aitken, J.D., Su,
912 Y., Chassaing, B., Walters, W.A., Gonzalez, A.*, et al.* (2012). Transient inability to manage
913 proteobacteria promotes chronic gut inflammation in TLR5-deficient mice. Cell Host Microbe
914 *12*, 139-152.
915 Chassaing, B., and Darfeuille-Michaud, A. (2011). The commensal microbiota and
916 enteropathogens in the pathogenesis of inflammatory bowel diseases. Gastroenterology *140*,
917 1720-1728.
918 Chassaing, B., and Darfeuille-Michaud, A. (2013). The sigmaE pathway is involved in biofilm
919 formation by Crohn's disease-associated adherent-invasive Escherichia coli. J Bacteriol *195*, 76-
920 84.
921 Chassaing, B., Etienne-Mesmin, L., Bonnet, R., and Darfeuille-Michaud, A. (2013). Bile salts
922 induce long polar fimbriae expression favouring Crohn's disease-associated adherent-invasive
923 Escherichia coli interaction with Peyer's patches. Environ Microbiol *15*, 355-371.

924 Chassaing, B., Garenaux, E., Carriere, J., Rolhion, N., Guerardel, Y., Barnich, N., Bonnet, R.,
925 and Darfeuille-Michaud, A. (2015a). Analysis of sigmaE regulon in Crohn disease-associated E.
926 coli revealed waaWVL operon involved in biofilm formation. J Bacteriol.
927 Chassaing, B., and Gewirtz, A.T. (2014). Gut microbiota, low-grade inflammation, and
928 metabolic syndrome. Toxicol Pathol *42*, 49-53.
929 Chassaing, B., and Gewirtz, A.T. (2016). Has provoking microbiota aggression driven the
930 obesity epidemic? Bioessays *38*, 122-128.
931 Chassaing, B., and Gewirtz, A.T. (2018). Mice harboring pathobiont-free microbiota do not
932 develop intestinal inflammation that normally results from an innate immune deficiency. PLoS
933 One *13*, e0195310.
934 Chassaing, B., and Gewirtz, A.T. (2019). Identification of Inner Mucus-Associated Bacteria by
935 Laser Capture Microdissection. Cell Mol Gastroenterol Hepatol *7*, 157-160.
936 Chassaing, B., Koren, O., Carvalho, F.A., Ley, R.E., and Gewirtz, A.T. (2014a). AIEC
937 pathobiont instigates chronic colitis in susceptible hosts by altering microbiota composition. Gut
938 *63*, 1069-1080.
939 Chassaing, B., Koren, O., Goodrich, J.K., Poole, A.C., Srinivasan, S., Ley, R.E., and Gewirtz,
940 A.T. (2015b). Dietary emulsifiers impact the mouse gut microbiota promoting colitis and
941 metabolic syndrome. Nature *519*, 92-96.
942 Chassaing, B., Ley, R.E., and Gewirtz, A.T. (2014b). Intestinal epithelial cell toll-like receptor 5
943 regulates the intestinal microbiota to prevent low-grade inflammation and metabolic syndrome in
944 mice. Gastroenterology *147*, 1363-1377 e1317.

945 Chassaing, B., Miles-Brown, J., Pellizzon, M., Ulman, E., Ricci, M., Zhang, L., Patterson, A.D.,
946 Vijay-Kumar, M., and Gewirtz, A.T. (2015c). Lack of soluble fiber drives diet-induced adiposity
947 in mice. Am J Physiol Gastrointest Liver Physiol *309*, G528-541.
948 Chassaing, B., Raja, S.M., Lewis, J.D., Srinivasan, S., and Gewirtz, A.T. (2017a). Colonic
949 Microbiota Encroachment Correlates With Dysglycemia in Humans. Cell Mol Gastroenterol
950 Hepatol *4*, 205-221.
951 Chassaing, B., Rolhion, N., de Vallee, A., Salim, S.Y., Prorok-Hamon, M., Neut, C., Campbell,
952 B.J., Soderholm, J.D., Hugot, J.P., Colombel, J.F.*, et al.* (2011a). Crohn disease--associated
953 adherent-invasive E. coli bacteria target mouse and human Peyer's patches via long polar
954 fimbriae. J Clin Invest *121*, 966-975.
955 Chassaing, B., Rolhion, N., Vallee, A., Salim, S.Y., Prorok-Hamon, M., Neut, C., Campbell,
956 B.J., Soderholm, J.D., Hugot, J.P., Colombel, J.F.*, et al.* (2011b). Crohn disease-associated
957 adherent-invasive E. coli bacteria target mouse and human Peyer's patches via long polar
958 fimbriae. J Clin Invest *121*, 966-975.
959 Chassaing, B., Srinivasan, G., Delgado, M.A., Young, A.N., Gewirtz, A.T., and Vijay-Kumar,
960 M. (2012). Fecal lipocalin 2, a sensitive and broadly dynamic non-invasive biomarker for
961 intestinal inflammation. PLoS One *7*, e44328.
962 Chassaing, B., Van de Wiele, T., De Bodt, J., Marzorati, M., and Gewirtz, A.T. (2017b). Dietary
963 emulsifiers directly alter human microbiota composition and gene expression ex vivo
964 potentiating intestinal inflammation. Gut *66*, 1414-1427.
965 Cox, S., Sandall, A., Smith, L., Rossi, M., and Whelan, K. (2020). Food additive emulsifiers: a
966 review of their role in foods, legislation and classifications, presence in food supply, dietary
967 exposure, and safety assessment. Nutr Rev.

968 Darfeuille-Michaud, A., Boudeau, J., Bulois, P., Neut, C., Glasser, A.L., Barnich, N., Bringer,
969 M.A., Swidsinski, A., Beaugerie, L., and Colombel, J.F. (2004). High prevalence of adherent-
970 invasive Escherichia coli associated with ileal mucosa in Crohn's disease. Gastroenterology *127*,
971 412-421.
972 Duprey, A., Reverchon, S., and Nasser, W. (2014). Bacterial virulence and Fis: adapting
973 regulatory networks to the host environment. Trends Microbiol *22*, 92-99.
974 Edgar, R.C. (2010). Search and clustering orders of magnitude faster than BLAST.
975 Bioinformatics *26*, 2460-2461.
976 EFSA (2015). Scientific Opinion on the re-evaluation of polyoxyethylene sorbitan monolaurate
977 (E 432), polyoxyethylene sorbitan monooleate (E 433), polyoxyethylene sorbitan monopalmitate
978 (E 434), polyoxyethylene sorbitan monostearate (E 435) and polyoxyethylene sorbitan tristearate
979 (E 436) as food additives. EFSA Journal *13*, 1-74.
980 EFSA (2017). Re-evaluation of celluloses E 460(i), E 460(ii), E 461, E 462, E 463, E 464, E 465,
981 E 466, E 468 and E 469 as food additives. EFSA Journal *16*, 1-104.
982 Fang, F.C., Frawley, E.R., Tapscott, T., and Vazquez-Torres, A. (2016). Bacterial Stress
983 Responses during Host Infection. Cell Host Microbe *20*, 133-143.
984 Franchi, L., Amer, A., Body-Malapel, M., Kanneganti, T.D., Ozoren, N., Jagirdar, R., Inohara,
985 N., Vandenabeele, P., Bertin, J., Coyle, A.*, et al.* (2006). Cytosolic flagellin requires Ipaf for
986 activation of caspase-1 and interleukin 1beta in salmonella-infected macrophages. Nat Immunol
987 *7*, 576-582.
988 Gilbert, J.A., Meyer, F., Jansson, J., Gordon, J., Pace, N., Tiedje, J., Ley, R., Fierer, N., Field, D.,
989 Kyrpides, N.*, et al.* (2010). The Earth Microbiome Project: Meeting report of the "1 EMP

meeting on sample selection and acquisition" at Argonne National Laboratory October 6 2010. Stand Genomic Sci *3*, 249-253.

Glasser, A.L., Boudeau, J., Barnich, N., Perruchot, M.H., Colombel, J.F., and Darfeuille-Michaud, A. (2001). Adherent invasive Escherichia coli strains from patients with Crohn's disease survive and replicate within macrophages without inducing host cell death. Infection and immunity *69*, 5529-5537.

Gomes-Neto, J.C., Mantz, S., Held, K., Sinha, R., Segura Munoz, R.R., Schmaltz, R., Benson, A.K., Walter, J., and Ramer-Tait, A.E. (2017). A real-time PCR assay for accurate quantification of the individual members of the Altered Schaedler Flora microbiota in gnotobiotic mice. J Microbiol Methods *135*, 52-62.

Greten, F.R., Eckmann, L., Greten, T.F., Park, J.M., Li, Z.W., Egan, L.J., Kagnoff, M.F., and Karin, M. (2004). IKKbeta links inflammation and tumorigenesis in a mouse model of colitis-associated cancer. Cell *118*, 285-296.

Hayashi, F., Smith, K.D., Ozinsky, A., Hawn, T.R., Yi, E.C., Goodlett, D.R., Eng, J.K., Akira, S., Underhill, D.M., and Aderem, A. (2001). The innate immune response to bacterial flagellin is mediated by Toll-like receptor 5. Nature *410*, 1099-1103.

Johansson, M.E., and Hansson, G.C. (2012). Preservation of mucus in histological sections, immunostaining of mucins in fixed tissue, and localization of bacteria with FISH. Methods Mol Biol *842*, 229-235.

Jubelin, G., Desvaux, M., Schuller, S., Etienne-Mesmin, L., Muniesa, M., and Blanquet-Diot, S. (2018). Modulation of Enterohaemorrhagic Escherichia coli Survival and Virulence in the Human Gastrointestinal Tract. Microorganisms *6*.

1012 Katakura, K., Lee, J., Rachmilewitz, D., Li, G., Eckmann, L., and Raz, E. (2005). Toll-like
1013 receptor 9-induced type I IFN protects mice from experimental colitis. J Clin Invest *115*, 695-
1014 702.
1015 Keyamura, K., Fujikawa, N., Ishida, T., Ozaki, S., Su'etsugu, M., Fujimitsu, K., Kagawa, W.,
1016 Yokoyama, S., Kurumizaka, H., and Katayama, T. (2007). The interaction of DiaA and DnaA
1017 regulates the replication cycle in E. coli by directly promoting ATP DnaA-specific initiation
1018 complexes. Genes Dev *21*, 2083-2099.
1019 Kuhn, R., Lohler, J., Rennick, D., Rajewsky, K., and Muller, W. (1993). Interleukin-10-deficient
1020 mice develop chronic enterocolitis. Cell *75*, 263-274.
1021 Langmead, B., and Salzberg, S.L. (2012). Fast gapped-read alignment with Bowtie 2. Nat
1022 Methods *9*, 357-359.
1023 Laudisi, F., Di Fusco, D., Dinallo, V., Stolfi, C., Di Grazia, A., Marafini, I., Colantoni, A.,
1024 Ortenzi, A., Alteri, C., Guerrieri, F.*, et al.* (2018). The food additive maltodextrin promotes
1025 endoplasmic reticulum stress-driven mucus depletion and exacerbates intestinal inflammation.
1026 Cell Mol Gastroenterol Hepatol.
1027 Levine, A., Wine, E., Assa, A., Sigall Boneh, R., Shaoul, R., Kori, M., Cohen, S., Peleg, S.,
1028 Shamaly, H., On, A.*, et al.* (2019). Crohn's Disease Exclusion Diet Plus Partial Enteral Nutrition
1029 Induces Sustained Remission in a Randomized Controlled Trial. Gastroenterology *157*, 440-450
1030 e448.
1031 Llewellyn, S.R., Britton, G.J., Contijoch, E.J., Vennaro, O.H., Mortha, A., Colombel, J.F.,
1032 Grinspan, A., Clemente, J.C., Merad, M., and Faith, J.J. (2018). Interactions Between Diet and
1033 the Intestinal Microbiota Alter Intestinal Permeability and Colitis Severity in Mice.
1034 Gastroenterology *154*, 1037-1046 e1032.

1035 Lozupone, C., Hamady, M., and Knight, R. (2006). UniFrac--an online tool for comparing
1036 microbial community diversity in a phylogenetic context. BMC Bioinformatics *7*, 371.
1037 Lozupone, C., and Knight, R. (2005). UniFrac: a new phylogenetic method for comparing
1038 microbial communities. Appl Environ Microbiol *71*, 8228-8235.
1039 McDonald, D., Price, M.N., Goodrich, J., Nawrocki, E.P., DeSantis, T.Z., Probst, A., Andersen,
1040 G.L., Knight, R., and Hugenholtz, P. (2012). An improved Greengenes taxonomy with explicit
1041 ranks for ecological and evolutionary analyses of bacteria and archaea. ISME J *6*, 610-618.
1042 Miles, J.P., Zou, J., Kumar, M.V., Pellizzon, M., Ulman, E., Ricci, M., Gewirtz, A.T., and
1043 Chassaing, B. (2017). Supplementation of Low- and High-fat Diets with Fermentable Fiber
1044 Exacerbates Severity of DSS-induced Acute Colitis. Inflamm Bowel Dis *23*, 1133-1143.
1045 Miquel, S., Peyretaillade, E., Claret, L., de Vallee, A., Dossat, C., Vacherie, B., Zineb el, H.,
1046 Segurens, B., Barbe, V., Sauvanet, P.*, et al.* (2010). Complete genome sequence of Crohn's
1047 disease-associated adherent-invasive E. coli strain LF82. PLoS One *5*.
1048 Ng, S.C., Shi, H.Y., Hamidi, N., Underwood, F.E., Tang, W., Benchimol, E.I., Panaccione, R.,
1049 Ghosh, S., Wu, J.C.Y., Chan, F.K.L.*, et al.* (2017). Worldwide incidence and prevalence of
1050 inflammatory bowel disease in the 21st century: a systematic review of population-based studies.
1051 Lancet.
1052 Nickerson, K.P., Homer, C.R., Kessler, S.P., Dixon, L.J., Kabi, A., Gordon, I.O., Johnson, E.E.,
1053 de la Motte, C.A., and McDonald, C. (2014). The dietary polysaccharide maltodextrin promotes
1054 Salmonella survival and mucosal colonization in mice. PLoS One *9*, e101789.
1055 Nickerson, K.P., and McDonald, C. (2012). Crohn's disease-associated adherent-invasive
1056 Escherichia coli adhesion is enhanced by exposure to the ubiquitous dietary polysaccharide
1057 maltodextrin. PLoS One *7*, e52132.

1058 Palmela, C., Chevarin, C., Xu, Z., Torres, J., Sevrin, G., Hirten, R., Barnich, N., Ng, S.C., and
1059 Colombel, J.F. (2018). Adherent-invasive Escherichia coli in inflammatory bowel disease. Gut
1060 *67*, 574-587.
1061 Price, M.N., Dehal, P.S., and Arkin, A.P. (2009). FastTree: computing large minimum evolution
1062 trees with profiles instead of a distance matrix. Mol Biol Evol *26*, 1641-1650.
1063 Roberts, C.L., Keita, A.V., Duncan, S.H., O'Kennedy, N., Soderholm, J.D., Rhodes, J.M., and
1064 Campbell, B.J. (2010). Translocation of Crohn's disease Escherichia coli across M-cells:
1065 contrasting effects of soluble plant fibres and emulsifiers. Gut *59*, 1331-1339.
1066 Roberts, C.L., Rushworth, S.L., Richman, E., and Rhodes, J.M. (2013). Hypothesis: Increased
1067 consumption of emulsifiers as an explanation for the rising incidence of Crohn's disease. J
1068 Crohns Colitis *7*, 338-341.
1069 Rodriguez-Palacios, A., Harding, A., Menghini, P., Himmelman, C., Retuerto, M., Nickerson,
1070 K.P., Lam, M., Croniger, C.M., McLean, M.H., Durum, S.K.*, et al.* (2018). The Artificial
1071 Sweetener Splenda Promotes Gut Proteobacteria, Dysbiosis, and Myeloperoxidase Reactivity in
1072 Crohn's Disease-Like Ileitis. Inflamm Bowel Dis *24*, 1005-1020.
1073 Rolhion, N., Carvalho, F.A., and Darfeuille-Michaud, A. (2007). OmpC and the sigma(E)
1074 regulatory pathway are involved in adhesion and invasion of the Crohn's disease-associated
1075 Escherichia coli strain LF82. Molecular microbiology *63*, 1684-1700.
1076 Sabino, J., Lewis, J.D., and Colombel, J.F. (2019). Treating Inflammatory Bowel Disease With
1077 Diet: A Taste Test. Gastroenterology *157*, 295-297.
1078 Sellon, R.K., Tonkonogy, S., Schultz, M., Dieleman, L.A., Grenther, W., Balish, E., Rennick,
1079 D.M., and Sartor, R.B. (1998). Resident enteric bacteria are necessary for development of

spontaneous colitis and immune system activation in interleukin-10-deficient mice. Infect Immun *66*, 5224-5231.

Sevrin, G., Massier, S., Chassaing, B., Agus, A., Delmas, J., Denizot, J., Billard, E., and Barnich, N. (2018). Adaptation of adherent-invasive E. coli to gut environment: impact on flagellum expression and bacterial colonization ability. Gut Microbes *in press*.

Suez, J., Korem, T., Zeevi, D., Zilberman-Schapira, G., Thaiss, C.A., Maza, O., Israeli, D., Zmora, N., Gilad, S., Weinberger, A.*, et al.* (2014). Artificial sweeteners induce glucose intolerance by altering the gut microbiota. Nature *514*, 181-186.

Tobacman, J.K. (2001). Review of harmful gastrointestinal effects of carrageenan in animal experiments. Environ Health Perspect *109*, 983-994.

Trapnell, C., Roberts, A., Goff, L., Pertea, G., Kim, D., Kelley, D.R., Pimentel, H., Salzberg, S.L., Rinn, J.L., and Pachter, L. (2012). Differential gene and transcript expression analysis of RNA-seq experiments with TopHat and Cufflinks. Nature protocols *7*, 562-578.

Vazeille, E., Chassaing, B., Buisson, A., Dubois, A., de Vallee, A., Billard, E., Neut, C., Bommelaer, G., Colombel, J.F., Barnich, N.*, et al.* (2016). GipA Factor Supports Colonization of Peyer's Patches by Crohn's Disease-associated Escherichia Coli. Inflamm Bowel Dis *22*, 68-81.

Viennois, E., and Chassaing, B. (2018). First victim, later aggressor: How the intestinal microbiota drives the pro-inflammatory effects of dietary emulsifiers? Gut Microbes, 1-4.

Viennois, E., Gewirtz, A.T., and Chassaing, B. (2019). Chronic Inflammatory Diseases: Are We Ready for Microbiota-based Dietary Intervention? Cell Mol Gastroenterol Hepatol *8*, 61-71.

Viennois, E., Merlin, D., Gewirtz, A.T., and Chassaing, B. (2017). Dietary Emulsifier-Induced Low-Grade Inflammation Promotes Colon Carcinogenesis. Cancer Res *77*, 27-40.

1102 Vijay-Kumar, M., Aitken, J.D., Carvalho, F.A., Cullender, T.C., Mwangi, S., Srinivasan, S.,
1103 Sitaraman, S.V., Knight, R., Ley, R.E., and Gewirtz, A.T. (2010). Metabolic syndrome and
1104 altered gut microbiota in mice lacking Toll-like receptor 5. Science *328*, 228-231.
1105 Xavier, R.J., and Podolsky, D.K. (2007). Unravelling the pathogenesis of inflammatory bowel
1106 disease. Nature *448*, 427-434.
1107 Zeevi, D., Korem, T., Zmora, N., Israeli, D., Rothschild, D., Weinberger, A., Ben-Yacov, O.,
1108 Lador, D., Avnit-Sagi, T., Lotan-Pompan, M.*, et al.* (2015). Personalized Nutrition by Prediction
1109 of Glycemic Responses. Cell *163*, 1079-1094.
1110 Zmora, N., Suez, J., and Elinav, E. (2019). You are what you eat: diet, health and the gut
1111 microbiota. Nat Rev Gastroenterol Hepatol *16*, 35-56.

1112

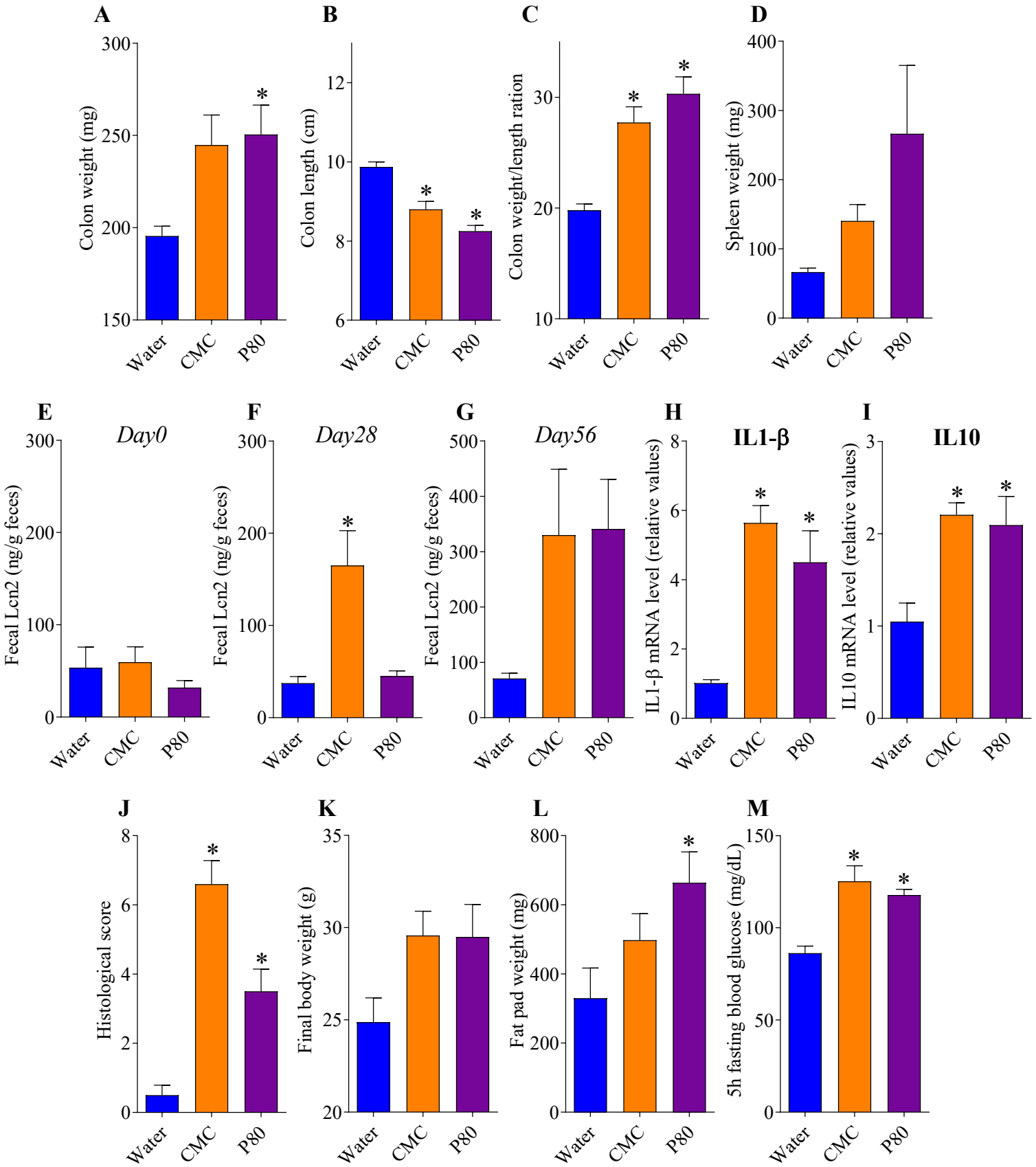

Figure 1: Colonization by adherent-invasive *Escherichia coli* bacteria is sufficient to promote detrimental effects of emulsifiers in normally protected ASF mice.

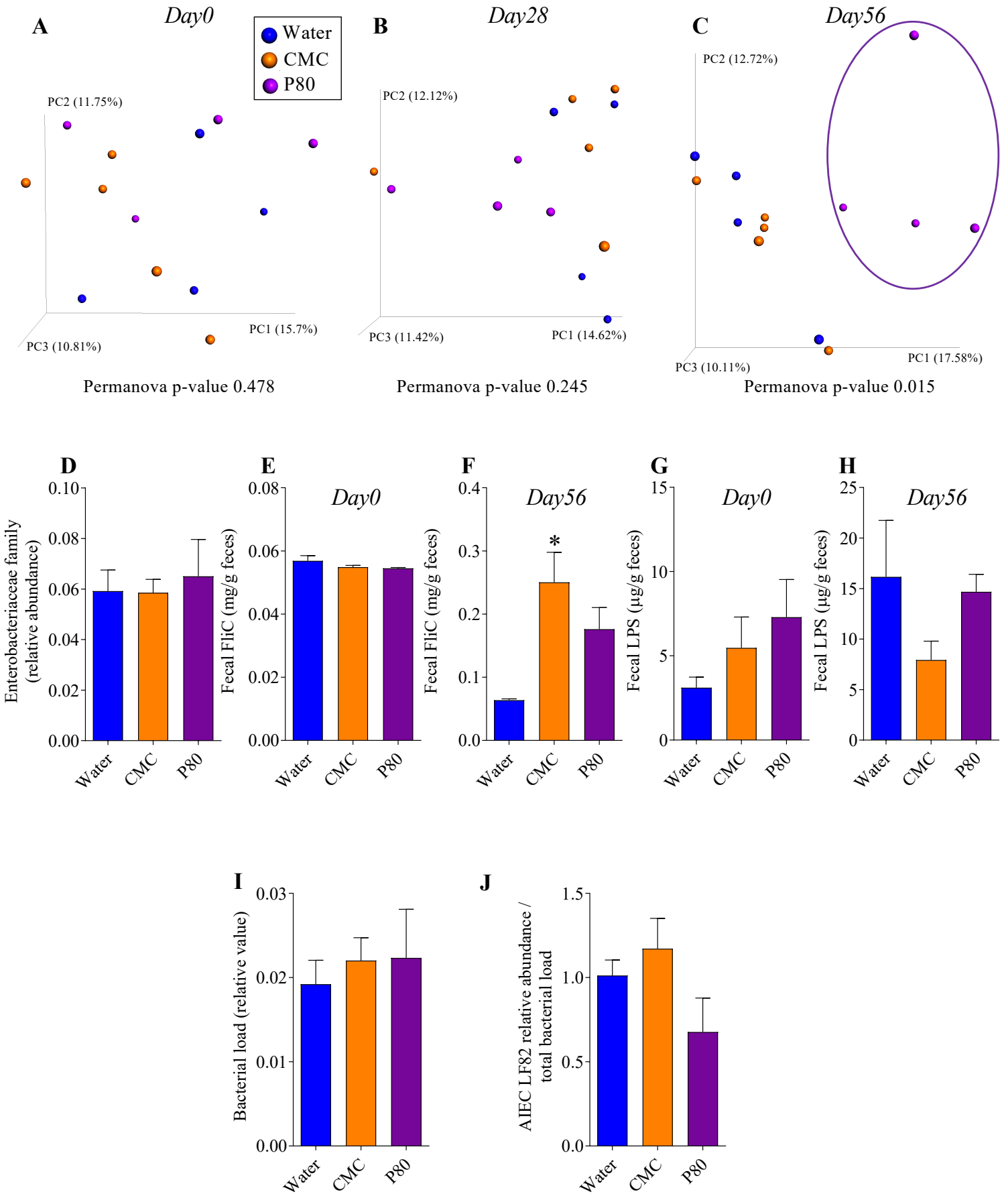

Figure 2: Colonization of ASF mice by adherent-invasive *Escherichia coli* bacteria is sufficient to induce emulsifier-mediated alterations in microbiota.

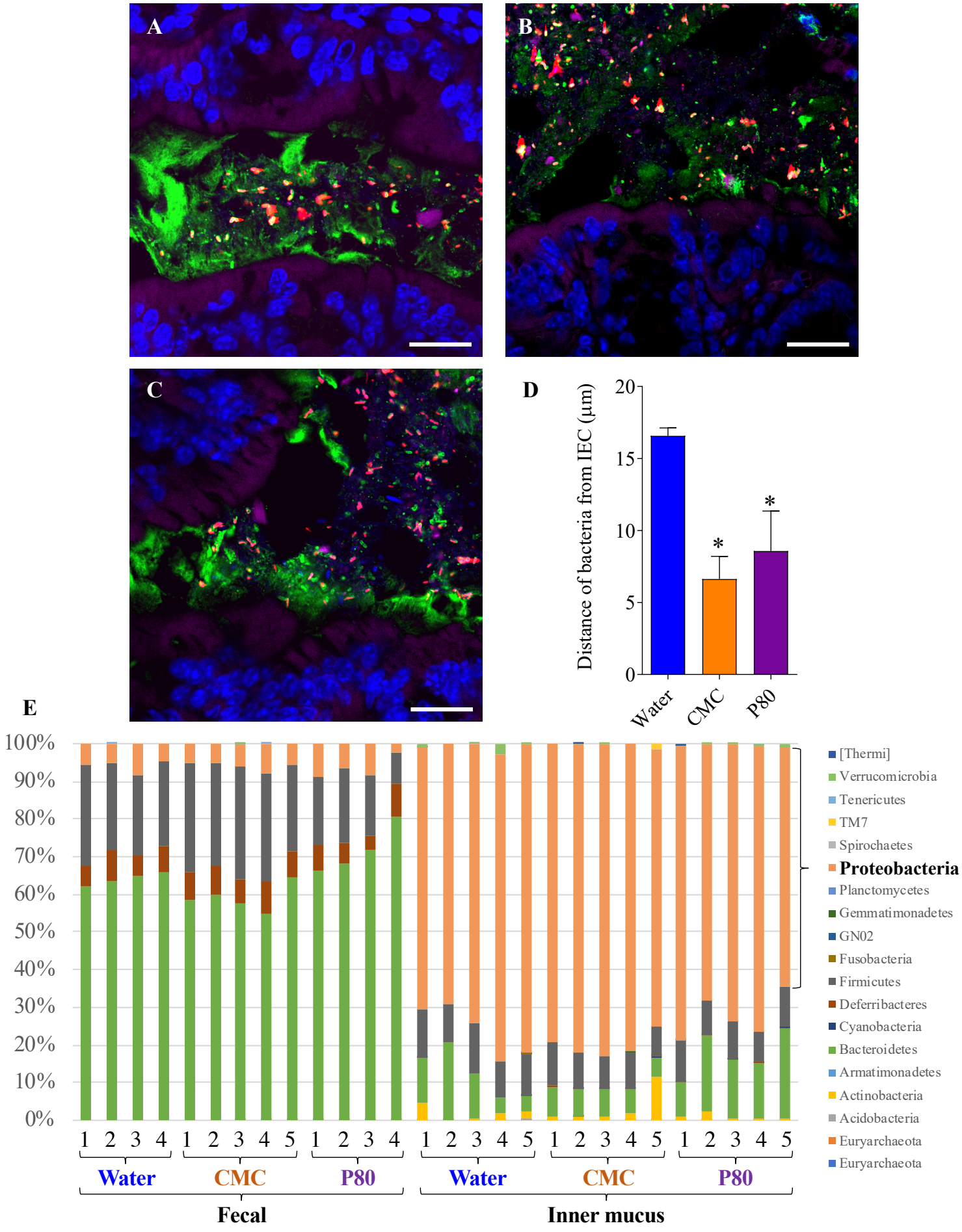

Figure 3: Colonization by adherent-invasive *Escherichia coli* bacteria is sufficient to induce microbiota encroachment in normally protected ASF mice.

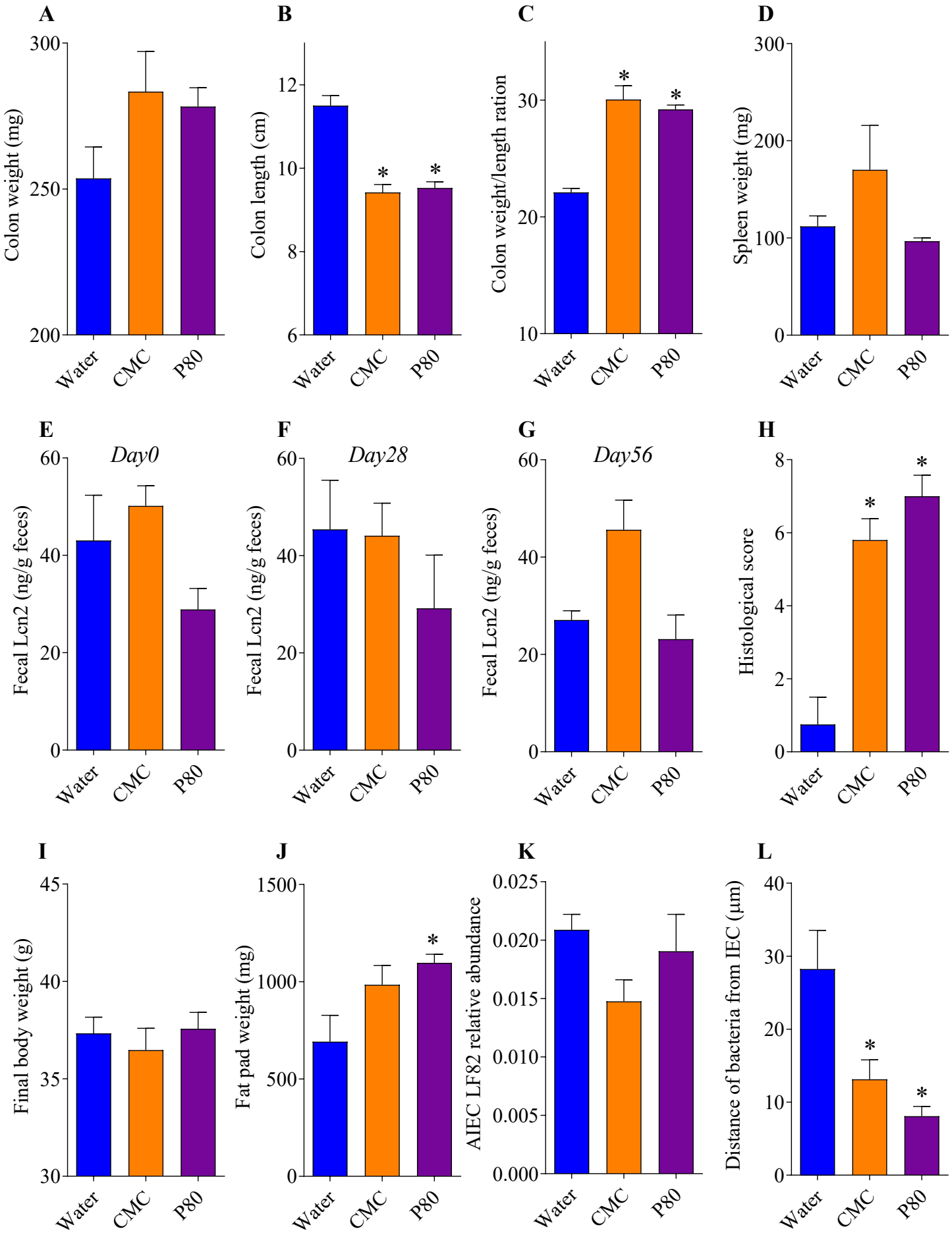

Figure 4: Mono-colonization by adherent-invasive *Escherichia coli* bacteria is sufficient to drive detrimental effects of emulsifiers in WT mice.

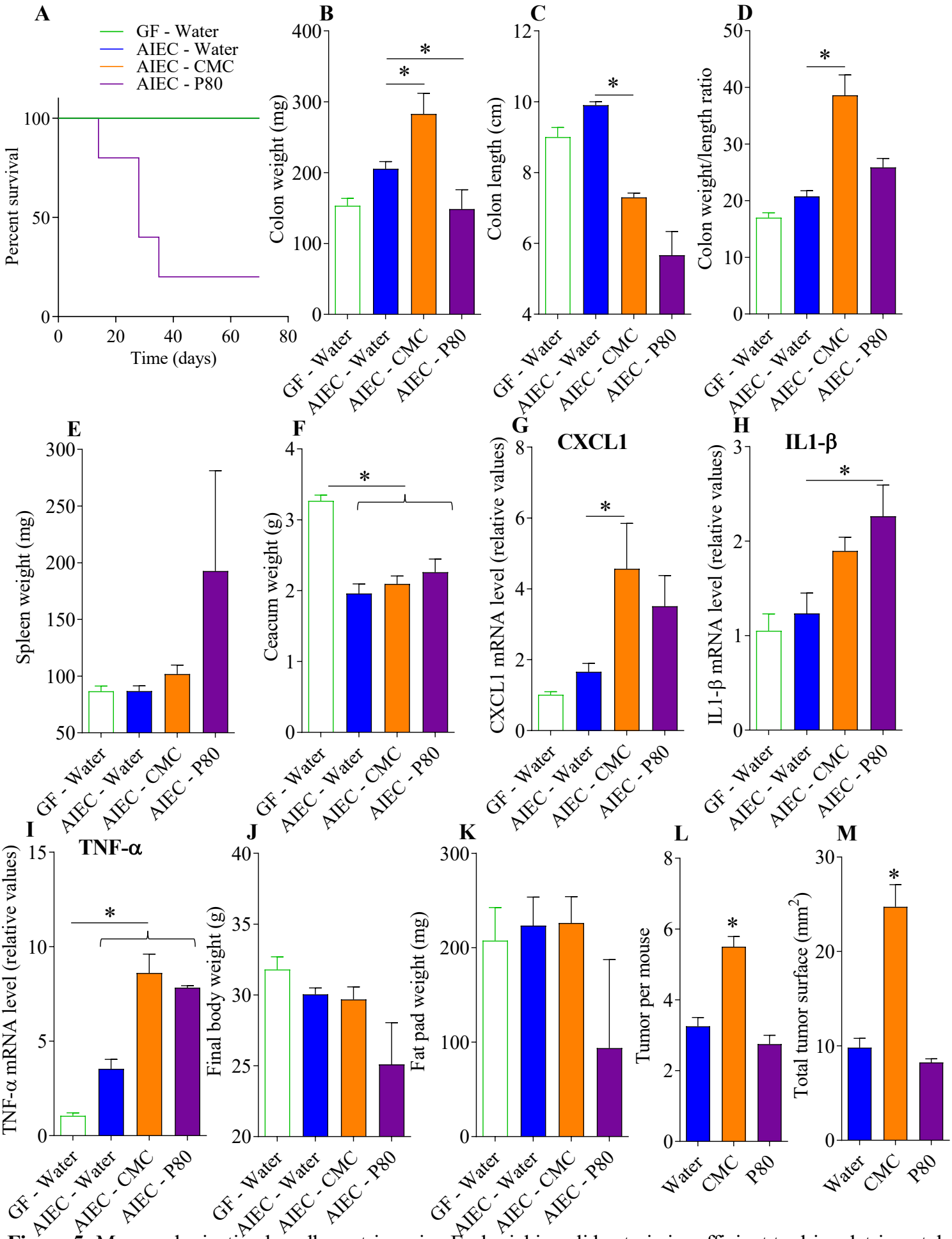

Figure 5: Mono-colonization by adherent-invasive Escherichia coli bacteria is sufficient to drive detrimental effects of emulsifiers in IL10-/- mice and promotion of colon cancer in WT.

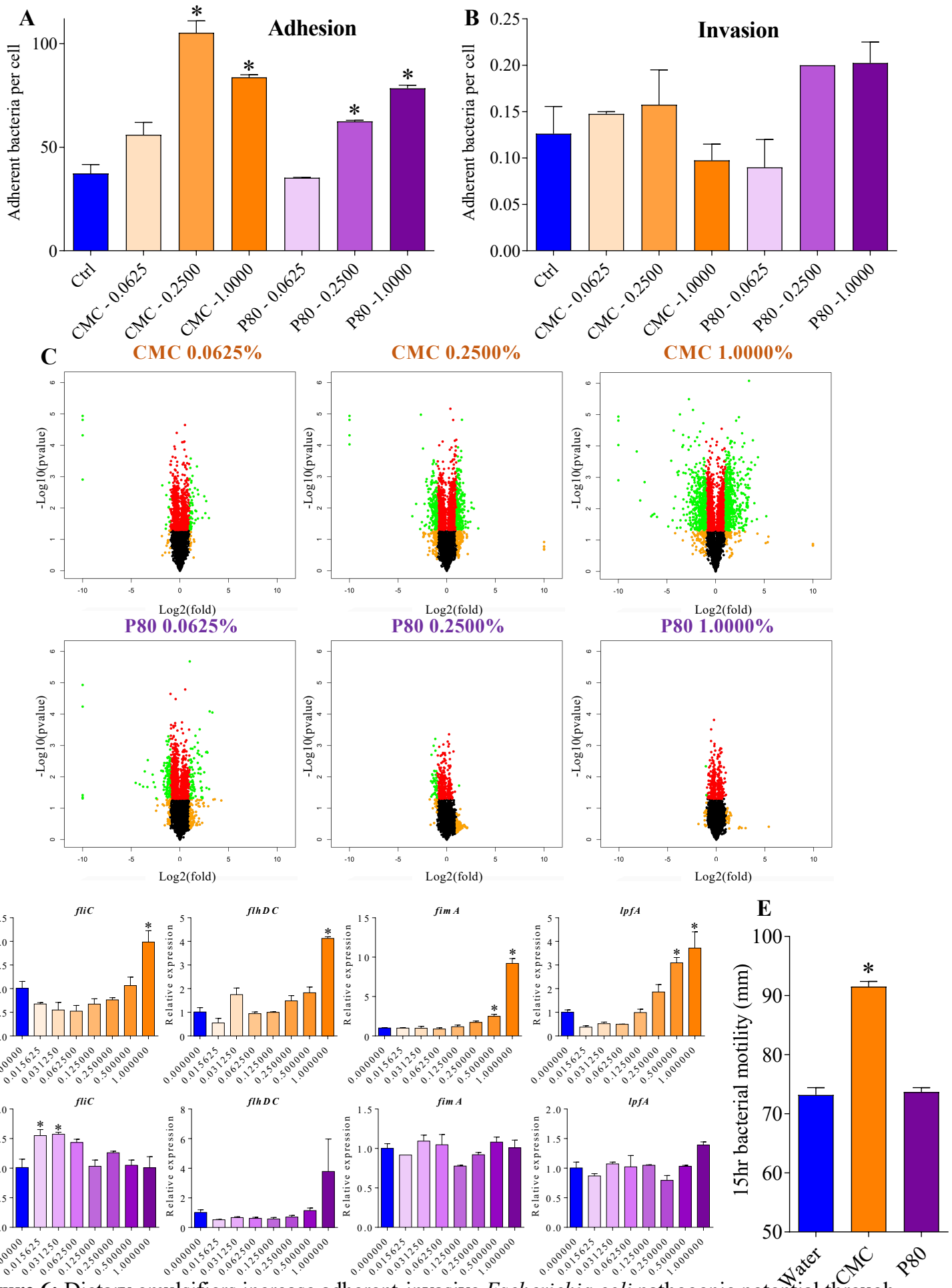

Figure 6: Dietary emulsifiers increase adherent-invasive *Escherichia coli* pathogenic potential through transcriptome modulation.

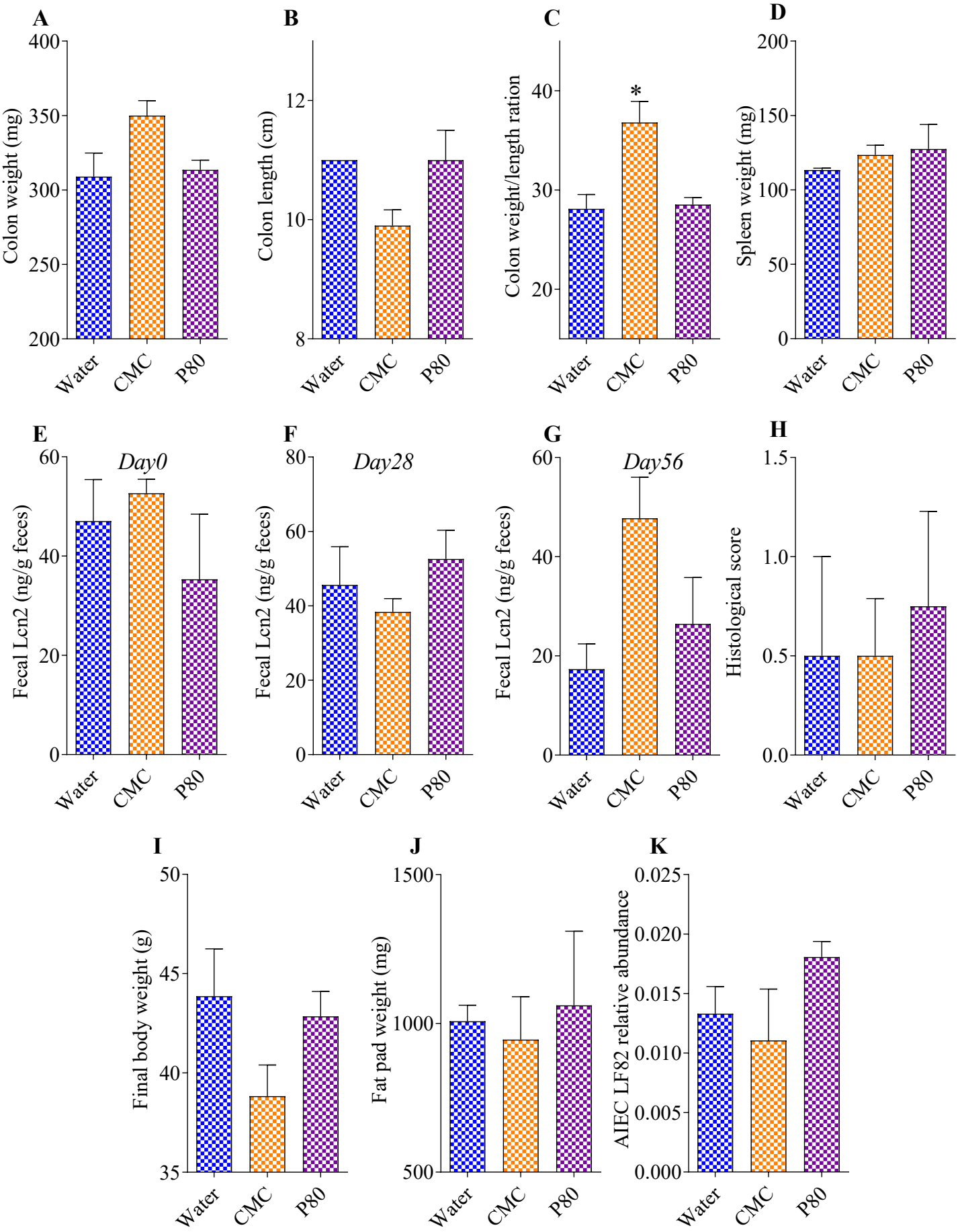

Figure 7: Bacterial flagellin contributes to AIEC-mediated emulsifier detrimental effects.

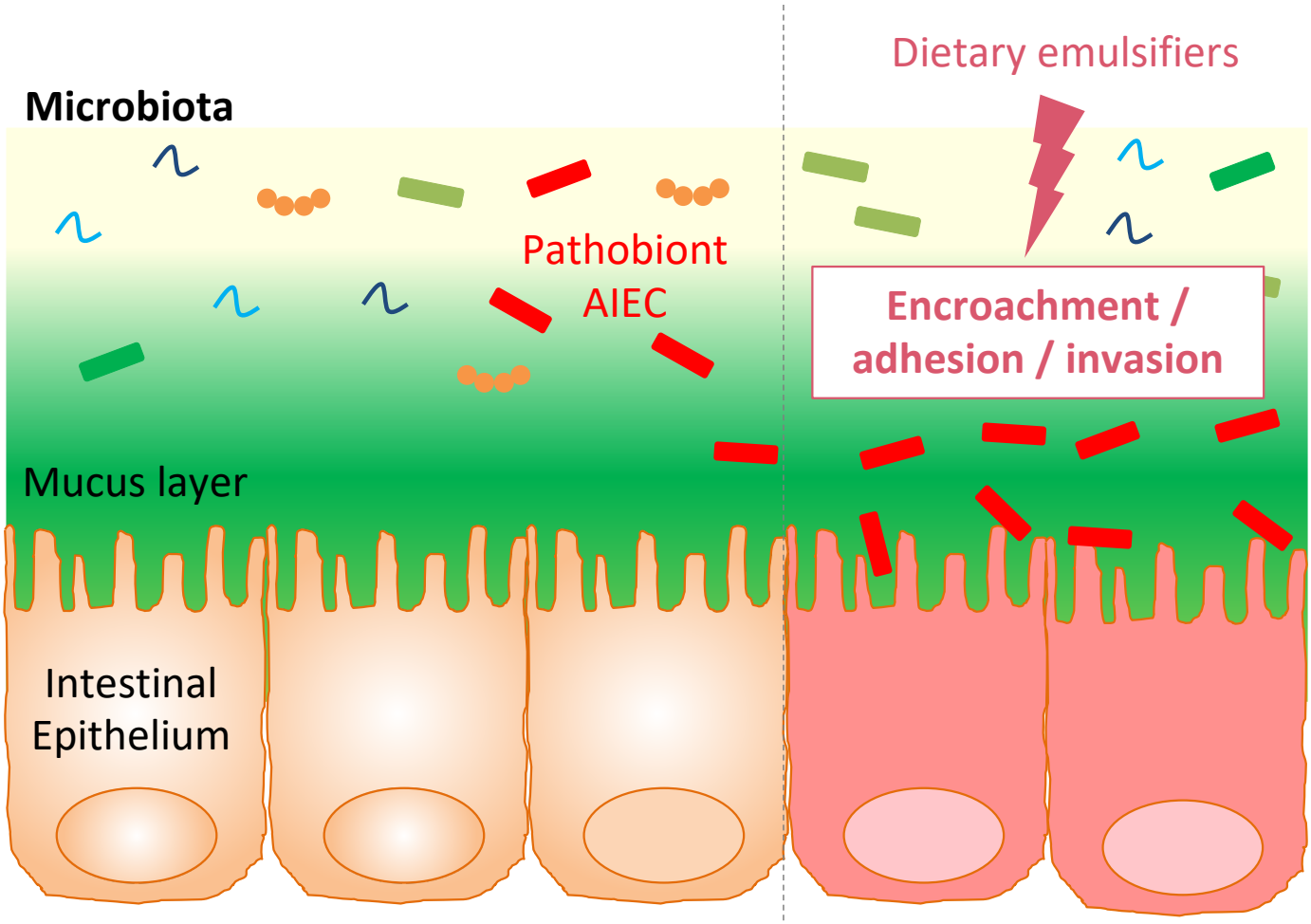

Chronic intestinal Inflammation

- *Colitis in genetically susceptible host*
- *Metabolic deregulations in WT host*
- *Promotion of colitis-associated cancer*